ФИЗИКА ЭЛЕМЕНТАРНЫХ ЧАСТИЦ И АТОМНОГО ЯДРА
2007. Т. 38. ВЫП. 4

EXACTLY SOLVABLE MODELS: THE WAY TOWARDS A RIGOROUS TREATMENT OF PHASE TRANSITIONS IN FINITE SYSTEMS

K. A. Bugaev

Bogolyubov Institute for Theoretical Physics, National Academy of Sciences of Ukraine, Kiev
Lawrence Berkeley National Laboratory, Berkeley, Ca, USA

ФИЗИКА ЭЛЕМЕНТАРНЫХ ЧАСТИЦ И АТОМНОГО ЯДРА
2007. Т. 38. ВЫП. 4

EXACTLY SOLVABLE MODELS: THE WAY TOWARDS A RIGOROUS TREATMENT OF PHASE TRANSITIONS IN FINITE SYSTEMS

K. A. Bugaev

Bogolyubov Institute for Theoretical Physics, National Academy of Sciences of Ukraine, Kiev
Lawrence Berkeley National Laboratory, Berkeley, Ca, USA

The exact analytical solutions of a variety of statistical models recently obtained for finite systems are thoroughly discussed. Among them are a constrained version of the statistical multifragmentation model, the Gas of Bags Model and the Hills and Dales Model of surface partition. The finite volume analytical solutions of these models were obtained by a novel powerful mathematical method — the Laplace–Fourier transform. Thus, the Laplace–Fourier transform allows one to study the nuclear matter equation of state, the equation of state of hadronic and quark–gluon plasma and the surface entropy of large clusters on the same footing. A complete analysis of the isobaric partition singularities of these models is done for finite systems. The developed formalism allows us, for the first time, to exactly define the finite volume analogs of gaseous, liquid and mixed phases of these models from the first principles of statistical mechanics and demonstrates the pitfalls of earlier works. The found solutions may be used for building up a new theoretical apparatus to rigorously study phase transitions in finite systems. The strategic directions of future research opened by these exact results are also discussed.

Подробно обсуждаются точные аналитические решения набора статистических моделей, полученных в последнее время для конечных систем, а именно: ограниченной версии статистической мультифрагментационной модели, модели газовых мешков и модели поверхностного деления Хиллса и Далеса. Аналитические решения ограниченного объема этих моделей получены с помощью оригинального мощного математического метода преобразования Лапласа–Фурье. Таким образом, преобразование Лапласа–Фурье позволяет исследовать уравнение состояния ядерной материи, уравнение состояния адронной и кварк-глюонной плазмы и поверхностную энтропию больших кластеров единым образом. Проведен полный анализ изобарных распределенных сингулярностей этих моделей для конечных систем. Развитый формализм впервые позволяет точно определить ограниченные по объему аналоги газообразной, жидкой и смешанной фаз этих моделей, исходя из первых принципов статистической механики, и показывает недостатки более ранних работ. Найденные решения могут быть использованы для построения нового теоретического аппарата для детального исследования фазовых переходов в конечных системах. Обсуждаются также стратегические направления будущих исследований, открывающиеся благодаря этим точным результатам.

PACS: 25.70. Pq, 21.65.+f, 24.10. Pa

1. THEORETICAL DESCRIPTION OF PHASE TRANSITIONS IN FINITE SYSTEMS

Investigation of the properties of strongly interacting matter under extreme conditions is one of the most important subjects of modern physics. Over the last

20 years, rich data on two phase transitions (PTs) existing in strongly interacting matter, the nuclear liquid–gas PT [1–3] and the deconfinement PT between the hadronic matter and quark–gluon plasma (QGP) [4], were collected by many experiments. However, despite this progress, the theoretical understanding of these PTs is far from being perfect. In part, this is because these PTs can be studied only in the collisions of finite nuclear systems at finite colliding energies. Under such conditions only a finite number of particles can be produced in the collision and, therefore, the traditional methods of statistical mechanics cannot be used for successful identification of these PTs, since a rigorous theory of critical phenomena in finite systems was not built up to now.

However, the experimental studies of PTs in nuclear systems demand the formulation of such a theory. In particular, the investigations of the above-mentioned nuclear liquid–gas PT [1–3] require the development of theoretical approaches which would allow us to study the critical phenomena without going into the thermodynamic limit $V \to \infty$ (V is the volume of the system), because such a limit does not exist due to the long range Coulomb interaction. Although at first glance the situation with the deconfinement PT looks better because the Coulomb interaction seems to be less important for it, the reality may prepare a few unpleasant surprises for us, when the well-established signals of the deconfinement PT [5, 6] will be studied in the collisions of small nuclei. Therefore, there is a great need in the theoretical approaches which may shed light on the «internal mechanism» of how the PTs happen in finite systems.

The general situation in the theory of critical phenomena for finite (small) systems is not very optimistic at the moment because theoretical progress in this field has been slow. It is well known that the mathematical theory of phase transitions was worked out by T. D. Lee and C. N. Yang [7]. Unfortunately, there is no direct generic relation between the physical observables and zeros of the grand canonical partition in a complex fugacity plane. Therefore, we know very well what are the gaseous and liquid phases at infinite volumes: mixture of fragments of all sizes and ocean, respectively. This is known both for pure phases and for their mixture, but, despite some limited success [8], this general approach is not useful for the specific problems of critical phenomena in finite systems (see Sec. 8 below).

The tremendous complexity of critical phenomena in finite systems prevented their systematic and rigorous theoretical study. For instance, even the best formulation of the statistical mechanics and thermodynamics of finite systems by Hill [9] is not rigorous while discussing PTs. As a result, the absence of a well-established definition of the liquid and mixed phases for finite volumes delays the progress of several related fields, including the theoretical and experimental searches for the reliable signals of several PTs which are expected to exist in strongly interacting matter. Therefore, *the task of the highest priority* of the theory of critical phenomena is *to define the finite volume analogs of phases from*

the first principles of statistical mechanics. At present, it is unclear whether such definitions can be made for a general case, but it turns out that such finite volume definitions can be formulated for a variety of realistic nonclassical (= non mean-field) statistical models which are successfully used in nuclear multifragmentation and in relativistic nuclear collisions. Although there is a great similarity between the statistical models employed in nuclear multifragmentation and in relativistic heavy-ion collisions, the present work will be mainly devoted to the discussion of the nuclear liquid–gas PT because it is simpler and because, we hope, it can directly be used to verify the theoretical ideas and concepts on how to rigorously introduce the finite volume analogs of phases.

About 25 years ago, when the theoretical foundations of nuclear multifragmentation were established, there was an illusion that the theoretical basis is simple and clear, and, therefore, we need only the data and models which will describe them. The analysis of finite volume systems has proven to be very difficult. However, there was a clear way out of troubles by making numerical codes that are able to describe the data. This is, of course, a common way to handle such problems and there were many successes achieved in this way [1–3, 10]. However, there is another side of the coin which tells us that our understanding did not change much since then. This is so because the numerical simulations of this level do not provide us with any proof. At best, they just demonstrate something. With time the number of codes increased, but the common theoretical approach was not developed. This led to a bitter result — there are many good guesses in the nuclear multifragmentation community, but, unfortunately, little analytical work to back up these expectations. As a result, the absence of a firm theoretical ground led to formulation of such highly speculative «signals» of the nuclear liquid-vapor PT as negative heat capacity [11,12], bimodality [13], which later on were disproved in Refs. [14] and [15], respectively.

Thus, there is a paradoxic situation: there are many experimental data and facts, but there is no a single theoretical approach which is able to describe them. Similar to the searches for quark–gluon plasma (QGP) [16] there is lack of a firm and rigorous theoretical approach to describe phase transitions in finite systems.

However, our understanding of the multifragmentation phenomenon [1–3] was improved recently, when an exact analytical solution of a simplified version of the statistical multifragmentation model (SMM) [17,18] was found in [19,20]. These analytical results not only allowed us to understand the important role of the Fisher exponent τ on the phase structure of the nuclear liquid–gas PT and the properties of its (tri)critical point, but also to calculate the critical indices $\alpha', \beta, \gamma', \delta$ of the SMM [21] as functions of index τ. The determination of the simplified SMM exponents allowed us to show explicitly [21] that, in contrast to expectations, *the scaling relations for critical indices of the SMM differ from the corresponding relations of a well-known Fisher droplet model (FDM)* [22]. This exact analytical solution allowed us to predict a narrow range of values,

$1.799 < \tau < 1.846$, which, in contrast to FDM value $\tau_{\rm FDM} \approx 2.16$, is consistent with ISiS Collaboration data [23] and EOS Collaboration data [24]. This finding is not only of a principal theoretical importance, since it allows one to find out the universality class of the nuclear liquid–gas phase transition, if τ index can be determined from experimental mass distribution of fragments, but also it enhanced a great activity in extracting the value of τ exponent from the data [25, 26].

It is necessary to stress that such results *in principle* cannot be obtained either within the widely used mean-filed approach or numerically. This is the reason why exactly solvable models with phase transitions play a special role in statistical mechanics — they are the benchmarks of our understanding of critical phenomena that occur in more complicated substances. They are our theoretical laboratories, where we can study the most fundamental problems of critical phenomena which cannot be studied elsewhere. Their great advantage compared to other methods is that they provide us with the information obtained directly from the first principles of statistical mechanics being unspoiled by mean-field or other simplifying approximations without which the analytical analysis is usually impossible. On the other hand, an exact analytical solution gives the physical picture of PT, which cannot be obtained by numerical evaluation. Therefore, one can expect that an extension of the exact analytical solutions to finite systems may provide us with the ultimate and reliable experimental signals of the nuclear liquid–vapor PT which are established on a firm theoretical ground of statistical mechanics. This, however, is a very difficult general task of the critical-phenomena theory in finite systems.

Fortunately, we do not need to solve this very general task, but to find its solution for a specific problem of nuclear liquid–gas PT, which is less complicated and more realistic. In this case the straightforward way is to start from a few statistical models, like FDM and/or SMM, which are successful in describing the most of the experimental data. A systematic study of the various modifications of the FDM for finite volumes was performed by Moretto and collaborators [27], and it led to a discovery of thermal reducibility of the fragment charge spectra [3], to a determination of a quantitative liquid–vapor phase diagram containing the coexistence line up to critical temperature for small systems [28, 29], to the generalization of the FDM for finite systems and to a formulation of the complement concept [30, 31] which allows one to account for finite size effects of (small) liquid drop on the properties of its vapor. However, such a systematic analysis for the SMM was not possible until recently, when its finite volume analytical solution was found in [32].

An invention of a new powerful mathematical method [32], the Laplace–Fourier transform, is a major theoretical breakthrough in the statistical mechanics of finite systems of the last decade because it allowed us to solve exactly not only the simplified SMM for finite volumes [32], but also a variety of statistical surface partitions for finite clusters [33, 34] and to find out their surface entropy

and to shed light on a source of the Fisher exponent τ. It was shown [32] that for finite volumes the analysis of the grand canonical partition (GCP) of the simplified SMM is reduced to the analysis of the simple poles of the corresponding isobaric partition, obtained as a Laplace–Fourier transform of the GCP. Such a representation of the GCP allows one not only to show from the first principles that for finite systems there exist the complex values of the effective chemical potential, but also to define the finite volume analogs of phases straightforwardly. Moreover, this method allows one to include into consideration all complicated features of the interaction (including the Coulomb one) which have been neglected in the simplified SMM because it was originally formulated for infinite nuclear matter. Consequently, the Laplace–Fourier transform method opens a principally new possibility of studying the nuclear liquid–gas phase transition directly from the partition of finite system without taking its thermodynamic limit. Now this method is also applied [35] to the finite volume formulation of the Gas of Bags Model (GBM) [36] which is used to describe the PT between the hadronic matter and QGP. Thus, the Laplace–Fourier transform method not only gives an analytical solution for a variety of statistical models with PTs in finite volumes, but also provides us with a common framework for several critical phenomena in strongly interacting matter. Therefore, it turns out that further applications and developments of this method are very promising and important not only for the nuclear multifragmentation community, but also for several communities studying PTs in finite systems because this method may provide them with the firm theoretical foundations and a common theoretical language.

It is necessary to remember that further progress of this approach and its extension to other communities cannot be successfully achieved without new theoretical ideas about formalism itself and its applications to the data measured in low and high energy nuclear collisions. Both of these require essential and coherent efforts of a few theoretical groups working on the theory of PTs in finite systems, which, according to our best knowledge, do not exist at the moment either in multifragmentation community or elsewhere. Therefore, *the second task of the highest priority is to attract young and promising theoretical students* to these theoretical problems and create the necessary manpower to solve the up coming problems. Otherwise the negative consequences of a complete dominance of experimental groups and numerical codes will never be overcome and a good chance to build up a common theoretical apparatus for a few PTs will be lost forever. If this will be the case, then an essential part of the nuclear physics associated with nuclear multifragmentation will have no chance to survive in the next years.

Therefore, the first necessary step to resolve these two tasks of the highest priority is to formulate the up-to-date achievements of the exactly solvable models and to discuss the strategy for their further developments and improvements along with their possible impact on transport and hydrodynamic approaches. For these

reasons the paper is organized as follows: In Sec. 2 we formulate the simplified SMM and present its analytical solution in thermodynamic limit; in Sec. 3 we discuss the necessary conditions for PT of the given order and their relation to the singularities of the isobaric partition and apply these findings to the simplified SMM; Sec. 4 is devoted to the SMM critical indices as the functions of the Fisher exponent τ and their scaling relations; the Laplace–Fourier transform method is presented in Sec. 5 along with an exact analytical solution of the simplified SMM which has a constraint on the size of the largest fragment, whereas the analysis of its isobaric partition singularities and the meaning of the complex values of free energy are given in Sec. 6; Secs. 7 and 8 are devoted to the discussion of the case without PT and with it, respectively; at the end of Sec. 8 there is a discussion of the Chomaz and Gulminelli approach to bimodality [8]; in Sec. 9 we discuss the finite volume modifications of the Gas of Bags, i.e., the statistical model describing the PT between hadrons and QGP, whereas in Sec. 10 we formulate the Hills and Dales Model for the surface partition and present the limit of the vanishing amplitudes of deformations; and, finally, in Sec. 11 we discuss the strategy of future research which is necessary to build up a truly microscopic kinetics of phase transitions in finite systems.

2. STATISTICAL MULTIFRAGMENTATION IN THERMODYNAMIC LIMIT

The system states in the SMM are specified by the multiplicity sets $\{n_k\}$ ($n_k = 0, 1, 2, \ldots$) of k-nucleon fragments. The partition function of a single fragment with k nucleons is [1]: $V\phi_k(T) = V(mTk/2\pi)^{3/2} z_k$, where $k = 1, 2, \ldots, A$ (A is the total number of nucleons in the system), V and T are, respectively, the volume and the temperature of the system, m is the nucleon mass. The first two factors on the right-hand side (r.h.s.) of the single fragment partition originate from the nonrelativistic thermal motion and the last factor, z_k, represents the intrinsic partition function of the k-nucleon fragment. Therefore, the function $\phi_k(T)$ is a phase space density of the k-nucleon fragment. For $k = 1$ (nucleon) we take $z_1 = 4$ (4 internal spin-isospin states) and for fragments with $k > 1$ we use the expression motivated by the liquid-drop model (see details in [1]): $z_k = \exp(-f_k/T)$, with fragment free energy

$$f_k = -W(T)k + \sigma(T)k^{2/3} + (\tau + 3/2)T \ln k, \tag{1}$$

with $W(T) = W_0 + T^2/\epsilon_0$. Here $W_0 = 16$ MeV is the bulk binding energy per nucleon. T^2/ϵ_0 is the contribution of the excited states taken in the Fermi-gas approximation ($\epsilon_0 = 16$ MeV); $\sigma(T)$ is the temperature-dependent surface tension parameterized in the following relation: $\sigma(T) = \sigma(T)|_{\mathrm{SMM}} \equiv \sigma_0[(T_c^2 - T^2)/(T_c^2 + T^2)]^{5/4}$, with $\sigma_0 = 18$ MeV and $T_c = 18$ MeV ($\sigma = 0$ at $T \geqslant T_c$). The

last contribution in Eq. (1) involves the famous Fisher term with dimensionless parameter τ. As will be shown later, at the critical (tricritical) point, the fragment mass distribution will lose its exponential form and will become a power law $k^{-\tau}$.

It is necessary to stress that the SMM parameterization of the surface tension coefficient is not a unique one. For instance, the FDM successfully employs another one $\sigma(T)|_{\rm FDM} = \sigma_0[1-T/T_c]$. As we shall see in Sec. 4, the temperature dependence of the surface tension coefficient in the vicinity of the critical point will define the critical indices of the model, but the following mathematical analysis of the SMM is general and is valid for an arbitrary $\sigma(T)$ function.

The canonical partition function (CPF) of nuclear fragments in the SMM has the following form:

$$Z_A^{\rm id}(V,T) = \sum_{\{n_k\}} \left[\prod_{k=1}^{A} \frac{[V\ \phi_k(T)]^{n_k}}{n_k!} \right] \delta(A - \sum_k k n_k). \qquad (2)$$

In Eq. (2), the nuclear fragments are treated as point-like objects. However, these fragments have nonzero proper volumes and they should not overlap in the coordinate space. In the excluded volume (Van der Waals) approximation this is achieved by substituting the total volume V in Eq. (2) by the free (available) volume $V_f \equiv V - b\sum_k k n_k$, where $b = 1/\rho_0$ ($\rho_0 = 0.16$ fm^{-3} is the normal nuclear density). Therefore, the corrected CPF becomes: $Z_A(V,T) = Z_A^{\rm id}(V - bA, T)$. The SMM defined by Eq. (2) was studied numerically in [17,18]. This is a simplified version of the SMM, since the symmetry and Coulomb contributions are neglected. However, its investigation appears to be of principal importance for studies of the nuclear liquid–gas phase transition.

The calculation of $Z_A(V,T)$ is difficult due to the constraint $\sum_k k n_k = A$. This difficulty can be partly avoided by evaluating the grand canonical partition (GCP)

$$\mathcal{Z}(V,T,\mu) \equiv \sum_{A=0}^{\infty} \exp\left(\frac{\mu A}{T}\right) Z_A(V,T)\Theta(V - bA), \qquad (3)$$

where μ denotes a chemical potential. The calculation of $\mathcal{Z}$ is still rather difficult. The summation over $\{n_k\}$ sets in Z_A cannot be performed analytically because of additional A dependence in the free volume V_f and the restriction $V_f > 0$. The presence of the theta function in the GCP (3) guarantees that only configurations with positive value of the free volume are counted. However, similarly to the delta-function restriction in Eq. (2), it makes again the calculation of $\mathcal{Z}(V,T,\mu)$ (3) to be rather difficult. This problem was resolved [19, 20] by performing the Laplace transformation of $\mathcal{Z}(V,T,\mu)$. This introduces the so-called isobaric

partition function (IP) [36]:

$$\hat{\mathcal{Z}}(s,T,\mu) \equiv \int\limits_0^\infty dV\, \mathrm{e}^{-sV}\, \mathcal{Z}(V,T,\mu) =$$

$$= \int\limits_0^\infty dV'\, \mathrm{e}^{-sV'} \sum_{\{n_k\}} \prod_k \frac{1}{n_k!} \left\{ V' \phi_k(T)\, \exp\left[\frac{(\mu - sbT)k}{T} \right] \right\}^{n_k} =$$

$$= \int\limits_0^\infty dV'\, \mathrm{e}^{-sV'}\, \exp\left\{ V' \sum_{k=1}^\infty \phi_k\, \exp\left[\frac{(\mu - sbT)k}{T} \right] \right\}. \quad (4)$$

After changing the integration variable $V \to V'$, the constraint of Θ function has disappeared. Then all n_k were summed independently leading to the exponential function. Now the integration over V' in Eq. (4) can be done resulting in

$$\hat{\mathcal{Z}}(s,T,\mu) = \frac{1}{s - \mathcal{F}(s,T,\mu)}, \quad (5)$$

where

$$\mathcal{F}(s,T,\mu) = \sum_{k=1}^\infty \phi_k\, \exp\left[\frac{(\mu - sbT)k}{T} \right] =$$

$$= \left(\frac{mT}{2\pi} \right)^{3/2} \left[z_1\, \exp\left(\frac{\mu - sbT}{T} \right) + \sum_{k=2}^\infty k^{-\tau}\, \exp\left(\frac{(\tilde{\mu} - sbT)k - \sigma k^{2/3}}{T} \right) \right]. \quad (6)$$

Here we have introduced the shifted chemical potential $\tilde{\mu} \equiv \mu + W(T)$. From the definition of pressure in the grand canonical ensemble it follows that, in the thermodynamic limit, the GCP of the system behaves as

$$p(T,\mu) \equiv T \lim_{V\to\infty} \frac{\ln\, \mathcal{Z}(V,T,\mu)}{V} \Rightarrow \mathcal{Z}(V,T,\mu)\big|_{V\to\infty} \sim \exp\left[\frac{p(T,\mu)V}{T} \right]. \quad (7)$$

An exponentially over V increasing part of $\mathcal{Z}(V,T,\mu)$ on the right-hand side of Eq. (7) generates the rightmost singularity s^* of the function $\hat{\mathcal{Z}}(s,T,\mu)$, because for $s < p(T,\mu)/T$ the V integral for $\hat{\mathcal{Z}}(s,T,\mu)$ (4) diverges at its upper limit. Therefore, in the thermodynamic limit, $V \to \infty$, the system pressure is defined by this rightmost singularity, $s^*(T,\mu)$, of IP $\hat{\mathcal{Z}}(s,T,\mu)$ (4):

$$p(T,\mu) = T s^*(T,\mu). \quad (8)$$

Note that this simple connection of the rightmost s singularity of $\hat{\mathcal{Z}}$, Eq. (4), to the asymptotic, $V \to \infty$, behavior of $\mathcal{Z}$, Eq. (7), is a general mathematical

property of the Laplace transform. Due to this property, the study of the system behavior in the thermodynamic limit $V \to \infty$ can be reduced to the investigation of the singularities of $\hat{\mathcal{Z}}$.

3. SINGULARITIES OF ISOBARIC PARTITION AND PHASE TRANSITIONS

The IP, Eq. (4), has two types of singularities: 1) the simple pole singularity defined by the equation

$$s_g(T,\mu) = \mathcal{F}(s_g, T, \mu), \tag{9}$$

2) the singularity of the function $\mathcal{F}(s,T,\mu)$ itself at the point s_l, where the coefficient in linear over k terms in the exponent is equal to zero,

$$s_l(T,\mu) = \frac{\tilde{\mu}}{Tb}. \tag{10}$$

The simple pole singularity corresponds to the gaseous phase, where pressure is determined by the equation

$$p_g(T,\mu) = \left(\frac{mT}{2\pi}\right)^{3/2} T\left[z_1 \exp\left(\frac{\mu - bp_g}{T}\right) + \right.$$
$$\left. + \sum_{k=2}^{\infty} k^{-\tau} \exp\left(\frac{(\tilde{\mu} - bp_g)k - \sigma k^{2/3}}{T}\right)\right]. \tag{11}$$

The singularity $s_l(T,\mu)$ of the function $\mathcal{F}(s,T,\mu)$ (6) defines the liquid pressure

$$p_l(T,\mu) \equiv T s_l(T,\mu) = \frac{\tilde{\mu}}{b}. \tag{12}$$

In the considered model the liquid phase is represented by an infinite fragment, i.e., it corresponds to the macroscopic population of the single mode $k = \infty$. Here one can see the analogy with the Bose condensation, where the macroscopic population of a single mode occurs in the momentum space.

In the (T,μ) regions, where $\tilde{\mu} < bp_g(T,\mu)$, the gas phase dominates ($p_g > p_l$), while the liquid phase corresponds to $\tilde{\mu} > bp_g(T,\mu)$. The liquid–gas phase transition occurs when two singularities coincide, i.e., $s_g(T,\mu) = s_l(T,\mu)$. A schematic view of singular points is shown in Fig. 1, *a* for $T < T_c$, i.e., when $\sigma > 0$. The two-phase coexistence region is therefore defined by the equation

$$p_l(T,\mu) = p_g(T,\mu), \quad \text{i.e.,} \quad \tilde{\mu} = bp_g(T,\mu). \tag{13}$$

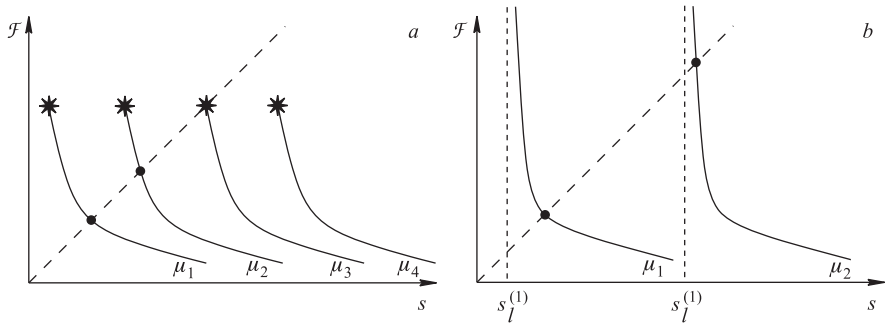

Fig. 1. Schematic view of singular points of the isobaric partition, Eq. (5), at $T < T_c$ (*a*) and $T > T_c$ (*b*). Solid lines show $\mathcal{F}(s, T, \mu)$ as a function of s at fixed T and μ, $\mu_1 < \mu_2 < \mu_3 < \mu_4$. Dots and asterisks indicate the simple poles (s_g) and the singularity of function $\mathcal{F}$ itself (s_l), respectively. At $\mu_3 = \mu^*(T)$ the two singular points coincide signaling a phase transition

One can easily see that $\mathcal{F}(s, T, \mu)$ is monotonously decreasing function of s. The necessary condition for the phase transition is that this function remains finite in its singular point $s_l = \tilde{\mu}/Tb$:

$$\mathcal{F}(s_l, T, \mu) < \infty. \tag{14}$$

The convergence of $\mathcal{F}$ is determined by τ and σ. At $\tau = 0$, the condition (14) requires $\sigma(T) > 0$. Otherwise, $\mathcal{F}(s_l, T, \mu) = \infty$ and the simple pole singularity $s_g(T, \mu)$ (9) is always the rightmost s singularity of $\hat{\mathcal{Z}}$ (4) (see Fig. 1, *b*). At $T > T_c$, where $\sigma(T)|_{\rm SMM} = 0$, the considered system can exist only in the one-phase state. It will be shown below that for $\tau > 1$ the condition (14) can be satisfied even at $\sigma(T) = 0$.

At $T < T_c$ the system undergoes the 1st order phase transition across the line $\mu^* = \mu^*(T)$ defined by Eq. (13). Its explicit form is given by the expression:

$$\mu^*(T) = -W(T) + \left(\frac{mT}{2\pi}\right)^{3/2} \times \\ \times Tb \left[z_1 \, \exp\left(-\frac{W(T)}{T}\right) + \sum_{k=2}^{\infty} k^{-\tau} \, \exp\left(-\frac{\sigma k^{2/3}}{T}\right) \right]. \tag{15}$$

The points on the line $\mu^*(T)$ correspond to the mixed phase states. First we consider the case $\tau = -1.5$ because it is the standard SMM choice.

The baryonic density is found as $(\partial p/\partial \mu)_T$ and is given by the following formulae in the liquid and gas phases:

$$\rho_l \equiv \left(\frac{\partial p_l}{\partial \mu}\right)_T = \frac{1}{b}, \qquad \rho_g \equiv \left(\frac{\partial p_g}{\partial \mu}\right)_T = \frac{\rho_{\rm id}}{1 + b\,\rho_{\rm id}}, \tag{16}$$

respectively. Here the function $\rho_{\rm id}$ is defined as

$$\rho_{\rm id}(T,\mu) = \left(\frac{mT}{2\pi}\right)^{3/2} \left[z_1 \exp\left(\frac{\mu - bp_g}{T}\right) + \right.$$
$$\left. + \sum_{k=2}^{\infty} k^{1-\tau} \exp\left(\frac{(\tilde{\mu} - bp_g)k - \sigma k^{2/3}}{T}\right)\right]. \quad (17)$$

Due to the condition (13) this expression is simplified in the mixed phase:

$$\rho_{\rm id}^{\rm mix}(T) \equiv \rho_{\rm id}(T, \mu^*(T)) =$$
$$= \left(\frac{mT}{2\pi}\right)^{3/2} \left[z_1 \exp\left(-\frac{W(T)}{T}\right) + \sum_{k=2}^{\infty} k^{1-\tau} \exp\left(-\frac{\sigma k^{2/3}}{T}\right)\right]. \quad (18)$$

This formula clearly shows that the bulk (free) energy acts in favor of the composite fragments, but the surface term favors single nucleons.

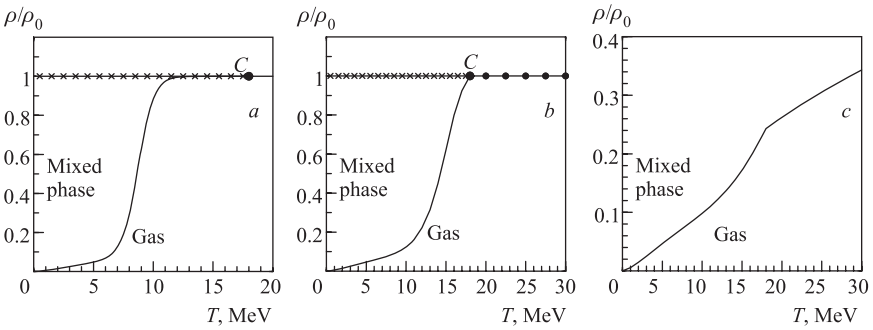

Fig. 2. Phase diagram in $T - \rho$ plane for $\tau = -1.5$ (*a*), $\tau = 1.1$ (*b*), and $\tau = 2.1$ (*c*). The mixed phase is represented by the extended region. Liquid phase (shown by crosses) exists at density $\rho = \rho_0$. Point C in *a* is the critical point, whereas in *b* it is the tricritical point. For $\tau > 2$ (*c*) the PT exists for all temperatures $T \geqslant 0$

Since at $\sigma > 0$ the sum in Eq. (18) converges at any τ, $\rho_{\rm id}$ is finite and according to Eq. (16) $\rho_g < 1/b$. Therefore, the baryonic density has a discontinuity $\Delta\rho = \rho_l - \rho_g > 0$ across the line $\mu^*(T)$ (15) for any τ. The discontinuities take place also for the energy and entropy densities. The phase diagram of the system in the (T, ρ) plane is shown in Fig. 2, *a*. The line $\mu^*(T)$ (15) corresponding to the mixed phase states is transformed into the finite region in the (T, ρ) plane. As usual, in this mixed phase region of the phase diagram the baryonic density ρ and the energy density are superpositions of the corresponding densities of liquid and gas:

$$\rho = \lambda\rho_l + (1-\lambda)\rho_g, \quad \varepsilon = \lambda\,\varepsilon_l + (1-\lambda)\varepsilon_g. \quad (19)$$

Here λ $(0 < \lambda < 1)$ is a fraction of the system volume occupied by the liquid inside the mixed phase, and the partial energy densities for $(i = l, g)$ can be found from the thermodynamic identity [19]:

$$\varepsilon_i \equiv T\frac{\partial p_i}{\partial T} + \mu\frac{\partial p_i}{\partial \mu} - p_i. \tag{20}$$

Inside the mixed phase at constant density ρ the parameter λ has a specific temperature dependence shown in the upper panel of Fig. 3, *a*: from an approximately constant value ρ/ρ_0 at small T the function $\lambda(T)$ drops to zero in a narrow vicinity of the boundary separating the mixed phase and the pure gaseous phase. This corresponds to a fast change of the configurations from the state which is dominated by one infinite liquid fragment to the gaseous multifragment configurations. It happens inside the mixed phase without discontinuities in the thermodynamical functions.

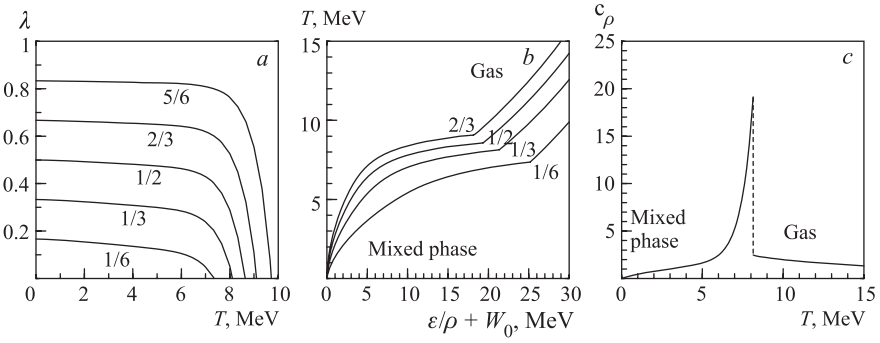

Fig. 3. *a*) Volume fraction $\lambda(T)$ of the liquid inside the mixed phase is shown as a function of temperature for fixed nucleon densities $\rho/\rho_0 = 1/6, 1/3, 1/2, 2/3, 5/6$ and $\tau = -1.5$. *b*) Temperature as a function of energy density per nucleon (caloric curve) is shown for fixed nucleon densities $\rho/\rho_0 = 1/6, 1/3, 1/2, 2/3$ and $\tau = -1.5$. Note that the shape of the model caloric curves is very similar to the experimental finding [37], although our estimates for the excitation energy are somewhat larger due to oversimplified interaction. For a quantitative comparison between the simplified SMM, the full SMM interaction should be accounted for. *c*) Specific heat per nucleon as a function of temperature at fixed nucleon density $\rho/\rho_0 = 1/3$. The dashed line shows the finite discontinuity of $c_\rho(T)$ at the boundary of the mixed and gaseous phases for $\tau = -1.5$

An abrupt decrease of $\lambda(T)$ near this boundary causes a strong increase of the energy density as a function of temperature. This is evident from Fig. 3, *b* which shows the caloric curves at different baryonic densities. One can clearly see a leveling of temperature at energies per nucleon between 10 and 20 MeV. As a consequence this leads to a sharp peak in the specific heat per nucleon at constant density, $c_\rho(T) \equiv (\partial\varepsilon/\partial T)_\rho/\rho$, presented in Fig. 3. A finite discontinuity

of $c_\rho(T)$ arises at the boundary between the mixed phase and the gaseous phase. This finite discontinuity is caused by the fact that $\lambda(T) = 0$, but $(\partial\lambda/\partial T)_\rho \neq 0$ at this boundary (see Fig. 3).

It should be emphasized that the energy density is continuous at the boundary of the mixed phase and the gaseous phase, hence the sharpness of the peak in c_ρ is entirely due to the strong temperature dependence of $\lambda(T)$ near this boundary. Moreover, at any $\rho < \rho_0$ the maximum value of c_ρ remains finite and the peak width in $c_\rho(T)$ is nonzero in the thermodynamic limit considered in our study. This is in contradiction with the expectation of [17, 18] that an infinite peak of zero width will appear in $c_\rho(T)$ in this limit. Also a comment about the so-called «boiling point» is appropriate here. This is a discontinuity in the energy density $\varepsilon(T)$ or, equivalently, a plateau in the temperature as a function of the excitation energy. Our analysis shows that this type of behavior indeed happens at constant pressure, but not at constant density! This is similar to the usual picture of a liquid–gas phase transition. In [17, 18] a rapid increase of the energy density as a function of temperature at fixed ρ near the boundary of the mixed and gaseous phases (see Fig. 3, *c*) was misinterpreted as a manifestation of the «boiling point».

New possibilities appear at nonzero values of the parameter τ. At $0 < \tau \leqslant 1$, the qualitative picture remains the same as discussed above, although there are some quantitative changes. For $\tau > 1$, the condition (14) is also satisfied at $T > T_c$, where $\sigma(T)|_{\mathrm{SMM}} = 0$. Therefore, the liquid–gas phase transition extends now to all temperatures. Its properties are, however, different for $\tau > 2$ and for $\tau \leqslant 2$ (see Fig. 2). If $\tau > 2$, the gas density is always lower than $1/b$ as ρ_{id} is finite. Therefore, the liquid–gas transition at $T > T_c$ remains the 1st order phase transition with discontinuities of baryonic density, entropy and energy densities (Fig. 2, *c*).

4. THE CRITICAL INDICES AND SCALING RELATIONS OF THE SMM

The above results allow one to find the critical exponents α', β, and γ' of the simplified SMM. These exponents describe the temperature dependence of the system near the critical point on the coexistence curve $\mu^* = \mu^*(T)$ (13), where the effective chemical potential $\nu \equiv \mu^*(T) + W(T) - bp(T, \mu^*(T)) = 0$ vanishes

$$c_\rho \sim \begin{cases} \mid \varepsilon \mid^{-\alpha}, & \text{for } \varepsilon < 0, \\ \varepsilon^{-\alpha'}, & \text{for } \varepsilon \geqslant 0, \end{cases} \tag{21}$$

$$\Delta\rho \sim \varepsilon^{\beta}, \quad \text{for } \varepsilon \geqslant 0, \tag{22}$$

$$\kappa_T \sim \varepsilon^{-\gamma'}, \quad \text{for } \varepsilon \geqslant 0, \tag{23}$$

where $\Delta\rho \equiv \rho_l - \rho_g$ defines the order parameter, $c_\rho \equiv \dfrac{T}{\rho}\left(\dfrac{\partial s}{\partial T}\right)_\rho$ denotes the specific heat at fixed particle density and $\kappa_T \equiv \dfrac{1}{\rho}\left(\dfrac{\partial \rho}{\partial p}\right)_T$ is the isothermal compressibility. The shape of the critical isotherm for $\rho \leqslant \rho_c$ is given by the critical index δ (the tilde indicates $\varepsilon = 0$ hereafter)

$$p_c - \tilde{p} \;\sim\; (\rho_c - \tilde{\rho})^\delta \quad \text{for } \varepsilon = 0. \tag{24}$$

The calculation of α and α' requires the specific heat c_ρ. With formula [39]

$$\frac{c_\rho(T,\mu)}{T} = \frac{1}{\rho}\left(\frac{\partial^2 p}{\partial T^2}\right)_\rho - \left(\frac{\partial^2 \mu}{\partial T^2}\right)_\rho \tag{25}$$

one obtains the specific heat on the PT curve by replacing the partial derivatives by the total ones [40]. The latter can be done for every state inside or on the boundary of the mixed phase region. For the chemical potential $\mu^*(T) = bp^*(T) - W(T)$ one gets $\dfrac{c^*_\rho(T)}{T} = \left(\dfrac{1}{\rho} - b\right)\dfrac{d^2p^*(T)}{dT^2} + \dfrac{d^2W(T)}{dT^2}$. Here the asterisk indicates the condensation line ($\nu = 0$) hereafter. Fixing $\rho = \rho_c = \rho_l = 1/b$, one finds $c^*_{\rho_l}(T) = T\dfrac{d^2W(T)}{dT^2}$ and, hence, obtains $\alpha = \alpha' = 0$. To calculate β, γ', and δ the behavior of the series

$$\Sigma_{\mathbf{q}}(\varepsilon,\nu) \equiv \sum_{k=2}^{\infty} k^{q-\tau}\,\exp\left(\frac{\nu}{T_c}k - A\varepsilon^\zeta k^\sigma\right) \tag{26}$$

should be analyzed for small positive values of ε and $-\nu$ ($A \equiv a_0/T_c$). In the limit $\varepsilon \to 0$ the function $\Sigma_{\mathbf{q}}(\varepsilon,0)$ remains finite, if $\tau > q+1$, and diverges otherwise. For $\tau = q+1$ this divergence is logarithmic. The case $\tau < q+1$ is analyzed in some detail, since even in Fisher's papers it was performed incorrectly.

With the substitution $\mathrm{z}_k \equiv k\left[A\varepsilon^\zeta\right]^{1/\sigma}$ one can prove [21] that in the limit $\varepsilon \to 0$ the series on the r. h. s. of (26) converges to an integral

$$\Sigma_q(\varepsilon,0) = \left[A\varepsilon^\zeta\right]^{\frac{\tau-q}{\sigma}} \sum_{k=2}^{\infty} z_k^{q-\tau}\,\mathrm{e}^{-z_k^\sigma} \to \left[A\varepsilon^\zeta\right]^{\frac{\tau-q-1}{\sigma}} \int\limits_{2[A\varepsilon^\zeta]^{1/\sigma}}^{\infty} dz z^{q-\tau}\,\mathrm{e}^{-z^\sigma}. \tag{27}$$

The assumption $q - \tau > -1$ is sufficient to guarantee the convergence of the integral at its lower limit. Using this representation, one finds the following

general results [21]

$$\Sigma_q(\varepsilon,0)\sim\begin{cases}\varepsilon^{\frac{\zeta}{\sigma}(\tau-q-1)}, & \text{if } \tau<q+1,\\ \ln\mid\varepsilon\mid, & \text{if } \tau=q+1,\\ \varepsilon^{0}, & \text{if } \tau>q+1,\end{cases}$$

and

$$\Sigma_q(0,\tilde{\nu})\sim\begin{cases}\tilde{\nu}^{\tau-q-1}, & \text{if } \tau<q+1,\\ \ln\mid\tilde{\nu}\mid, & \text{if } \tau=q+1,\\ \tilde{\nu}^{0}, & \text{if } \tau>q+1,\end{cases} \tag{28}$$

which allowed us to find out the critical indices of the SMM (see Table 1).

Table 1. **Critical exponents of the SMM and FDM as functions of the Fisher index τ for the general parameterization of the surface energy $\sigma(T)k^{2/3}\to\varepsilon^{\zeta}k^{\sigma}$ with $\varepsilon=(T_c-T)/T_c$**

Models	α'	α'_s	β	γ'	δ
SMM for $\tau<1+\sigma$	0	$2-\frac{\zeta}{\sigma}$	$\frac{\zeta}{\sigma}(2-\tau)$	$\frac{2\zeta}{\sigma}\left(\tau-\frac{3}{2}\right)$	$\frac{\tau-1}{2-\tau}$
SMM for $\tau\geqslant 1+\sigma$	0	$2-\frac{\zeta}{\sigma}(\sigma+2-\tau)$	$\frac{\zeta}{\sigma}(2-\tau)$	$\frac{2\zeta}{\sigma}\left(\tau-\frac{3}{2}\right)$	$\frac{\tau-1}{2-\tau}$
FDM	$2-\frac{\zeta}{\sigma}(\tau-1)$	N/A	$\frac{\zeta}{\sigma}(\tau-2)$	$\frac{\zeta}{\sigma}(3-\tau)$	$\frac{1}{\tau-2}$

In the special case $\zeta=2\sigma$, the well-known exponent inequalities proven for real gases by

$$\text{Fisher [36]:}\quad \alpha'+2\beta+\gamma'\geqslant 2, \tag{29}$$

$$\text{Griffiths [37]:}\quad \alpha'+\beta(1+\delta)\geqslant 2, \tag{30}$$

$$\text{Liberman [38]:}\quad \gamma'+\beta(1-\delta)\geqslant 0 \tag{31}$$

are fulfilled exactly for any τ. (The corresponding exponent inequalities for magnetic systems are often called Rushbrooke's, Griffiths', and Widom's inequalities, respectively.) For $\zeta>2\sigma$, Fisher's and Griffiths' exponent inequalities are fulfilled as inequalities and for $\zeta<2\sigma$ they are not fulfilled. The contradiction to Fisher's and Griffiths' exponent inequalities in this last case is not surprising. This is due to the fact that in the present version of the SMM the critical isochore $\rho=\rho_c=\rho_l$ lies on the boundary of the mixed phase to the liquid. Therefore, in expression (2.13) in [41] for the specific heat only the liquid phase contributes and, therefore, Fisher's proof of [41] following (2.13) cannot be applied for the SMM. Thus, the exponent inequalities (29) and (30) have to be modified for the SMM. Using results of Table 1, one finds the following scaling relations:

$$\alpha'+2\beta+\gamma'=\frac{\zeta}{\sigma}\quad\text{and}\quad\alpha'+\beta(1+\delta)=\frac{\zeta}{\sigma}. \tag{32}$$

Liberman's exponent inequality (31) is fulfilled exactly for any choice of ζ and σ.

Since the coexistence curve of the SMM is not symmetric with respect to $\rho = \rho_c$, it is interesting with regard to the specific heat to consider the difference $\Delta c_\rho(T) \equiv c^*_{\rho_g}(T) - c^*_{\rho_l}(T)$, following the suggestion of [40]. Using Eq. (25) for gas and liquid and noting that $1/\rho^*_g - b = 1/\rho^*_{\rm id}$, one obtains a specially defined index α'_s from the most divergent term for $\zeta > 1$

$$\Delta c_\rho(T) = \frac{T}{\rho^*_{\rm id}(T)} \frac{d^2 p^*(T)}{dT^2} \Rightarrow \alpha'_s = \begin{cases} 2 - \dfrac{\zeta}{\sigma}, & \text{if } \tau < \sigma + 1, \\ 2 - \dfrac{\zeta}{\sigma}(\sigma + 2 - \tau), & \text{if } \tau \geqslant \sigma + 1. \end{cases} \tag{33}$$

Then it is $\alpha'_s > 0$ for $\zeta/\sigma < 2$. Thus, approaching the critical point along any isochore within the mixed phase region except for $\rho = \rho_c = 1/b$, the specific heat diverges for $\zeta/\sigma < 2$ as defined by α'_s and remains finite for the isochore $\rho = \rho_c = 1/b$. This demonstrates the exceptional character of the critical isochore in this model.

In the special case that $\zeta = 1$ one finds $\alpha'_s = 2 - 1/\sigma$ for $\tau \leqslant 1 + 2\sigma$ and $\alpha'_s = -\beta$ for $\tau > 1 + 2\sigma$. Therefore, using α'_s instead of α', the exponent inequalities (29) and (30) are fulfilled exactly if $\zeta > 1$ and $\tau \leqslant \sigma + 1$ or if $\zeta = 1$ and $\tau \leqslant 2\sigma + 1$. In all other cases (29) and (30) are fulfilled as inequalities. Moreover, it can be shown that the SMM belongs to the universality class of real gases for $\zeta > 1$ and $\tau \geqslant \sigma + 1$.

The comparison of the above-derived formulae for the critical exponents of the SMM for $\zeta = 1$ with those obtained within the FDM (Eqs. (51)–(56) in [22]) shows that these models belong to different universality classes (except for the singular case $\tau = 2$).

Furthermore, one has to note that for $\zeta = 1, \sigma \leqslant 1/2$, and $1 + \sigma < \tau \leqslant 1 + 2\sigma$ the critical exponents of the SMM coincide with those of the exactly solved one-dimensional FDM with nonzero droplet-volumes [40].

For the usual parameterization of the SMM [1] one obtains with $\zeta = 5/4$ and $\sigma = 2/3$ the exponents

$$\alpha'_s = \begin{cases} \dfrac{1}{8}, & \text{if } \tau < \dfrac{5}{3} \\ \dfrac{15}{8}\tau - 3, & \text{if } \tau \geqslant \dfrac{5}{3}, \end{cases}$$
$$\beta = \frac{15}{8}(2 - \tau), \quad \gamma' = \frac{15}{4}\left(\tau - \frac{3}{2}\right), \quad \delta = \frac{\tau - 1}{2 - \tau}. \tag{34}$$

Thus, Fisher's suggestion to use α'_s instead of α' allows one to «*save*» *the exponential inequalities*, however, it is not a final solution of the problem.

The critical indices of the nuclear liquid–gas PT were determined from the multifragmentation of gold nuclei [44] and found to be close to those ones of real

gases. The method used to extract the critical exponents β and γ' in [44] was, however, found to have large uncertainties of about 25 per cent [45]. Nevertheless, those results allow us to estimate the value of τ from the experimental values of the critical exponents of real gases taken with large error bars. Using the above results we generalized [21] the exponent relations of [40]

$$\tau = 2 - \frac{\beta}{\gamma' + 2\beta} \quad \text{and} \quad \tau = 2 - \frac{1}{1+\delta} \tag{35}$$

for arbitrary σ and ζ. Then, one obtains with [46] $\beta = 0.32{-}0.39$, $\gamma' = 1.3{-}1.4$, and $\delta = 4{-}5$ the estimate $\tau = 1.799{-}1.846$. This demonstrates also that the value of τ is rather insensitive to the special choice of β, γ', and δ, which leads to $\alpha'_s \cong 0.373{-}0.461$ for the SMM. Theoretical values for β, γ', and δ for Ising-like systems within the renormalized ϕ^4 theory [47] lead to the narrow range $\tau = 1.828 \pm 0.001$. The values of β, γ', and δ indices for nuclear matter and percolation of two- and three-dimensional clusters are reviewed in [27].

There was a decent try to study the critical indices of the SMM numerically [48]. The version V2 of [48] corresponds precisely to our model with $\tau = 0$, $\zeta = 5/4$, and $\sigma = 2/3$, but their results contradict to our analysis. Their results for version V3 of [48] are in contradiction with our proof presented in [19]. There it was shown that for nonvanishing surface energy (as in version V3) the critical point does not exist at all. The latter was found in [48] for the finite system, and the critical indices were analyzed. Such a strange result, on the one hand, indicates that the numerical methods used in [48] are not self-consistent, and, on the other hand, it shows an indispensable value of the analytical calculations, which can be used as a test problem for numerical algorithms.

It is widely believed that the effective value of τ defined as $\tau_{\text{eff}} \equiv -\partial \ln n_k(\varepsilon)/\partial \ln k$ attains its minimum at the critical point (see references in [24]). This can be easily shown for the SMM. Indeed, taking the SMM fragment distribution $n_k(\varepsilon) = g(T)k^{-\tau} \exp\left[\frac{\nu}{T}k - \frac{a(\varepsilon)}{T}k^{\sigma}\right] \sim k^{-\tau_{\text{eff}}}$ one finds

$$\tau_{\text{eff}} = \tau - \frac{\nu}{T}k + \frac{\sigma a(\varepsilon)}{T}k^{\sigma} \Rightarrow \tau = \min(\tau_{\text{eff}}), \tag{36}$$

where the last step follows from the fact that the inequalities $a(\varepsilon) \geqslant 0$, $\nu \leqslant 0$ become equalities at the critical point $\nu = a(0) = 0$. Therefore, the SMM predicts that the minimal value of τ_{eff} corresponds to the critical point, where, as we see now, the mass distribution of fragments is power-like.

In the E900 $\pi^- + \text{Au}$ multifragmentation experiment [23] the ISiS Collaboration measured the dependence of τ_{eff} upon the excitation energy and found the

minimum value $\min(\tau_{\rm eff}) \cong 1.9$ (Fig. 5 of [23]). Also the EOS Collaboration [24] performed an analysis of the minimum of $\tau_{\rm eff}$ on Au + C multifragmentation data. The fitted $\tau_{\rm eff}$, plotted in Fig. 11, *b* of [24] versus the fragment multiplicity, exhibits a minimum in the range $\min(\tau_{\rm eff}) \cong 1.8-1.9$. Both results contradict the original FDM [22], but agree well with the above estimate of τ for real gases and for Ising-like systems in general.

5. CONSTRAINED SMM IN FINITE VOLUMES

Despite the great success, the application of the exact solution [19–21] to the description of experimental data is limited because this solution corresponds to an infinite system and due to that it cannot account for a more complicated interaction between nuclear fragments. Therefore, it was necessary to extend the exact solution [19–21] to finite volumes. It is clear that for the finite volume extension it is necessary to account for the finite size and geometrical shape of the largest fragments, when they are comparable with the system volume. For this one has to abandon the arbitrary size of the largest fragment and to consider the constrained SMM (CSMM) in which the largest fragment size is explicitly related to the volume V of the system.

Thus, the CSMM assumes a more strict constraint $\sum\limits_{k}^{K(V)} kn_k = A$, where the size of the largest fragment $K(V) = \alpha V/b$ cannot exceed the total volume of the system (the parameter $\alpha \leqslant 1$ is introduced for convenience). The case of the fixed size of the largest fragment, i.e., $K(V) = \text{const}$, analyzed numerically in [49] is also included in our treatment. A similar restriction should be also applied to the upper limit of the product in all partitions $Z_A^{\rm id}(V,T)$, $Z_A(V,T)$, and $\mathcal{Z}(V,T,\mu)$ introduced above (how to deal with the real values of $K(V)$, see later). Then the model with this constraint, the CSMM, cannot be solved by the Laplace transform method, because the volume integrals cannot be evaluated due to a complicated functional V dependence. However, the CSMM can be solved analytically with the help of the following identity [32]:

$$G(V) = \int\limits_{-\infty}^{+\infty} d\xi \int\limits_{-\infty}^{+\infty} \frac{d\eta}{2\pi}\, \mathrm{e}^{i\eta(V-\xi)} G(\xi), \tag{37}$$

which is based on the Fourier representation of the Dirac δ function. The representation (37) allows us to decouple the additional volume dependence and to reduce it to the exponential one, which can be dealt by the usual Laplace

transformation in the following sequence of steps:

$$\hat{\mathcal{Z}}(\lambda,T,\mu) \equiv \int\limits_0^\infty dV\ \mathrm{e}^{-\lambda V}\,\mathcal{Z}(V,T,\mu) = \int\limits_0^\infty dV' \int\limits_{-\infty}^{+\infty} d\xi \int\limits_{-\infty}^{+\infty} \frac{d\eta}{2\pi}\,\mathrm{e}^{i\eta(V'-\xi)-\lambda V'} \times$$

$$\times \sum_{\{n_k\}} \left[\prod_{k=1}^{K(\xi)} \frac{1}{n_k!} \left\{ V'\phi_k(T)\,\mathrm{e}\left(\frac{(\mu-(\lambda-i\eta)bT)k}{T} \right) \right\}^{n_k} \right] \Theta(V') =$$

$$= \int\limits_0^\infty dV' \int\limits_{-\infty}^{+\infty} d\xi \int\limits_{-\infty}^{+\infty} \frac{d\eta}{2\pi}\,\mathrm{e}^{i\eta(V'-\xi)-\lambda V'+V'\mathcal{F}(\xi,\lambda-i\eta)}. \quad (38)$$

After changing the integration variable $V \to V' = V - b\sum\limits_k^{K(\xi)} k\ n_k$, the constraint of Θ function has disappeared. Then all n_k were summed independently leading to the exponential function. Now the integration over V' in Eq. (38) can be straightforwardly done resulting in

$$\hat{\mathcal{Z}}(\lambda,T,\mu) = \int\limits_{-\infty}^{+\infty} d\xi \int\limits_{-\infty}^{+\infty} \frac{d\eta}{2\pi}\ \frac{\mathrm{e}^{-i\eta\xi}}{\lambda - i\eta - \mathcal{F}(\xi,\lambda-i\eta)}, \quad (39)$$

where the function $\mathcal{F}(\xi,\tilde{\lambda})$ is defined as follows:

$$\mathcal{F}(\xi,\tilde{\lambda}) = \sum_{k=1}^{K(\xi)} \phi_k(T)\ \exp\left(\frac{(\mu-\tilde{\lambda}bT)k}{T} \right) = \left(\frac{mT}{2\pi} \right)^{3/2} \times$$

$$\times \left[z_1\ \exp\left(\frac{\mu-\tilde{\lambda}bT}{T} \right) + \sum_{k=2}^{K(\xi)} k^{-\tau}\ \exp\left(\frac{(\mu+W-\tilde{\lambda}bT)k - \sigma k^{2/3}}{T} \right) \right]. \quad (40)$$

As usual, in order to find the GCP by the inverse Laplace transformation, it is necessary to study the structure of singularities of the isobaric partition (40).

6. ISOBARIC PARTITION SINGULARITIES AT FINITE VOLUMES

The isobaric partition (40) of the CSMM is, of course, more complicated than its SMM analog [19,20] because for finite volumes the structure of singularities in the CSMM is much richer than in the SMM, and they match in the limit $V \to \infty$

only. To see this let us first make the inverse Laplace transform:

$$\mathcal{Z}(V,T,\mu) = \int\limits_{\chi-i\infty}^{\chi+i\infty} \frac{d\lambda}{2\pi i}\hat{\mathcal{Z}}(\lambda,T,\mu)\,\mathrm{e}^{\lambda V} =$$

$$= \int\limits_{-\infty}^{+\infty} d\xi \int\limits_{-\infty}^{+\infty} \frac{d\eta}{2\pi} \int\limits_{\chi-i\infty}^{\chi+i\infty} \frac{d\lambda}{2\pi i}\, \frac{\mathrm{e}^{\lambda V - i\eta\xi}}{\lambda - i\eta - \mathcal{F}(\xi,\lambda-i\eta)} =$$

$$= \int\limits_{-\infty}^{+\infty} d\xi \int\limits_{-\infty}^{+\infty} \frac{d\eta}{2\pi}\,\mathrm{e}^{i\eta(V-\xi)} \sum_{\{\lambda_n\}} \mathrm{e}^{\lambda_n V}\left[1 - \frac{\partial\mathcal{F}(\xi,\lambda_n)}{\partial\lambda_n}\right]^{-1}, \quad (41)$$

nonindependent where the contour λ integral is reduced to the sum over the residues of all singular points $\lambda = \lambda_n + i\eta$ with $n = 1, 2, \ldots$, since this contour in the complex λ plane obeys the inequality $\chi > \max(\mathrm{Re}\,\{\lambda_n\})$. Now both remaining integrations in (41) can be done, and the GCP becomes

$$\mathcal{Z}(V,T,\mu) = \sum_{\{\lambda_n\}} \mathrm{e}^{\lambda_n V}\left[1 - \frac{\partial\mathcal{F}(V,\lambda_n)}{\partial\lambda_n}\right]^{-1}, \quad (42)$$

i.e., the double integral in (41) simply reduces to the substitution $\xi \to V$ in the sum over singularities. This is a remarkable result which was formulated in [32] as the following *theorem: if the Laplace–Fourier image of the excluded volume GCP exists, then for any additional V dependence of $\mathcal{F}(V,\lambda_n)$ or $\phi_k(T)$ the GCP can be identically represented by Eq. (42).*

The simple poles in (41) are defined by the equation

$$\lambda_n = \mathcal{F}(V,\lambda_n). \quad (43)$$

In contrast to the usual SMM [19,20] the singularities λ_n are (i) volume-dependent functions, if $K(V)$ is not constant, and (ii) they can have a nonzero imaginary part, but in this case there exist pairs of complex conjugate roots of (43) because the GCP is real.

Introducing the real R_n and imaginary I_n parts of $\lambda_n = R_n + iI_n$, we can rewrite Eq. (43) as a system of coupled transcendental equations

$$R_n = \sum_{k=1}^{K(V)} \tilde{\phi}_k(T)\,\exp\left(\frac{\mathrm{Re}\,(\nu_n)k}{T}\right)\cos\left(I_n bk\right), \quad (44)$$

$$I_n = -\sum_{k=1}^{K(V)} \tilde{\phi}_k(T)\,\exp\left(\frac{\mathrm{Re}\,(\nu_n)\,k}{T}\right)\sin\left(I_n bk\right), \quad (45)$$

where we have introduced the set of the effective chemical potentials $\nu_n \equiv \nu(\lambda_n)$ with $\nu(\lambda) = \mu + W(T) - \lambda bT$, and the reduced distribution functions $\tilde{\phi}_1(T) = \left(\frac{mT}{2\pi}\right)^{3/2} z_1 \exp\left(-W(T)/T\right)$ and $\tilde{\phi}_{k>1}(T) = \left(\frac{mT}{2\pi}\right)^{3/2} k^{-\tau} \times \exp\left(-\sigma(T)k^{2/3}/T\right)$ for convenience.

Consider the real root $(R_0 > 0, I_0 = 0)$, first. For $I_n = I_0 = 0$ the real root R_0 exists for any T and μ. Comparing of R_0 with the expression for vapor pressure of the analytical SMM solution [19, 20] shows that TR_0 is a constrained grand canonical pressure of the gas. As usual, for finite volumes the total mechanical pressure [9, 32] differs from TR_0. Equation (45) shows that for $I_{n>0} \neq 0$ the inequality $\cos\left(I_n bk\right) \leqslant 1$ never becomes the equality for all k values simultaneously. Then from Eq. (44) one obtains $(n > 0)$

$$R_n < \sum_{k=1}^{K(V)} \tilde{\phi}_k(T) \exp\left(\frac{\mathrm{Re}\left(\nu_n\right)k}{T}\right) \Rightarrow R_n < R_0, \tag{46}$$

where the second inequality (46) immediately follows from the first one. In other words, the gas singularity is always the rightmost one. This fact plays a decisive role in the thermodynamic limit $V \to \infty$.

The interpretation of the complex roots $\lambda_{n>0}$ is less straightforward. According to Eq. (42), the GCP is a superposition of the states of different free energies $-\lambda_n VT$. (Strictly speaking, $-\lambda_n VT$ has a meaning of the change of free energy, but we will use the traditional term for it.) For $n > 0$ the free energies are complex. Therefore, $-\lambda_{n>0}T$ is the density of free energy. The real part of the free energy density, $-R_nT$, defines the significance of the state's contribution to the partition: due to (46) the largest contribution always comes from the gaseous state and has the smallest real part of free energy density. As usual, the states which do not have the smallest value of the (real part of) free energy, i.e., $-R_{n>0}T$, are thermodynamically metastable. For infinite volume they should not contribute unless they are infinitesimally close to $-R_0T$, but for finite volumes their contribution to the GCP may be important.

As one sees from (44) and (45), the states of different free energies have different values of the effective chemical potential ν_n, which is not the case for infinite volume [19, 20], where there exists a single value for the effective chemical potential. Thus, for finite V the states which contribute to the GCP (42) are not in a true chemical equilibrium.

The meaning of the imaginary part of the free energy density becomes clear from (44) and (45) [50]: As one can see from (44) the imaginary part $I_{n>0}$ effectively changes the number of degrees of freedom of each k-nucleon fragment $(k \leqslant K(V))$ contribution to the free energy density $-R_{n>0}T$. It is clear, that the change of the effective number of degrees of freedom can occur virtually only

and if $\lambda_{n>0}$ state is accompanied by some kind of equilibration process. Both of these statements become clear, if we recall that the statistical operator in statistical mechanics and the quantum mechanical convolution operator are related by the Wick rotation [51]. In other words, the inverse temperature can be considered as an imaginary time. Therefore, depending on the sign, the quantity $I_n bT \equiv \tau_n^{-1}$, that appears in the trigonometric functions of equations (44) and (45) in front of the imaginary time $1/T$, can be regarded as the inverse decay/formation time τ_n of the metastable state which corresponds to the pole $\lambda_{n>0}$ (for more details see the next sections).

This interpretation of τ_n naturally explains the thermodynamic metastability of all states except the gaseous one: the metastable states can exist in the system only virtually because of their finite decay/formation time, whereas the gaseous state is stable because it has an infinite decay/formation time.

7. NO PHASE TRANSITION CASE

It is instructive to treat the effective chemical potential $\nu(\lambda)$ as an independent variable instead of μ. In contrast to the infinite V, where the upper limit $\nu \leqslant 0$ defines the liquid phase singularity of the isobaric partition and gives the pressure of a liquid phase $p_l(T,\mu) = TR_0|_{V\to\infty} = (\mu + W(T))/b$ [19, 20], for finite volumes and finite $K(V)$ the effective chemical potential can be complex (with either sign for its real part) and its value defines the number and position of the imaginary roots $\{\lambda_{n>0}\}$ in the complex plane. Positive and negative values of the effective chemical potential for finite systems were considered [38] within the Fisher droplet model, but, to our knowledge, its complex values have never been discussed. From the definition of the effective chemical potential $\nu(\lambda)$ it is evident that its complex values for finite systems exist only because of the excluded volume interaction, which is not taken into account in the Fisher droplet model [22]. However, a recent study of clusters of the $d = 2$ Ising model within the framework of FDM (see the corresponding section in [27]) shows that the excluded volume correction improves essentially the description of the thermodynamic functions. Therefore, the next step is to consider the complex values of the effective chemical potential and free energy for the excluded volume correction of the Ising clusters on finite lattices.

As is seen from Fig. 4, *a*, the r.h.s. of Eq. (45) is the amplitude and frequency modulated sine-like function of dimensionless parameter $I_n\, b$. Therefore, depending on T and $\mathrm{Re}\,(\nu)$ values, there may exist no complex roots $\{\lambda_{n>0}\}$, a finite number of them, or an infinite number of them. In Fig. 4, *b*, we showed a special case which corresponds to exactly three roots of Eq. (43) for each value of $K(V)$: the real root ($I_0 = 0$) and two complex conjugate roots ($\pm I_1$). Since the r.h.s. of (45) is monotonously increasing function of $\mathrm{Re}\,(\nu)$, when the former

is positive, it is possible to map the $T - \mathrm{Re}\,(\nu)$ plane into regions of a fixed number of roots of Eq. (43). Each curve in Fig. 4, *b* divides the $T - \mathrm{Re}\,(\nu)$ plane into three parts: for $\mathrm{Re}\,(\nu)$ values below the curve there is only one real root (gaseous phase), for points on the curve there exist three roots, and above the curve there are four or more roots of Eq. (43).

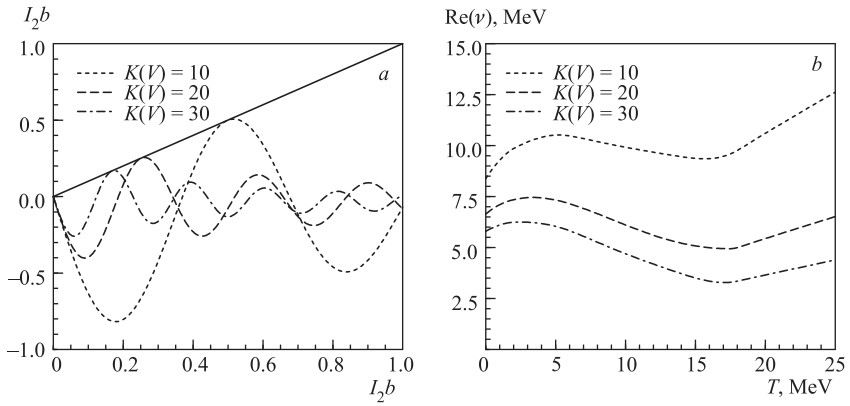

Fig. 4. *a*) A graphical solution of Eq. (45) for $T = 10$ MeV and $\tau = 1.825$. The l.h.s. (straight line) and r.h.s. of Eq. (45) (all dashed curves) are shown as the function of dimensionless parameter $I_2\, b$ for the three values of the largest fragment size $K(V)$. The intersection point at $(0;\, 0)$ corresponds to a real root of Eq. (43). Each tangent point with the straight line generates two complex roots of (43). *b*) Each curve separates the $T - \mathrm{Re}\,(\nu_n)$ region of one real root of Eq. (43) (below the curve), three complex roots (at the curve) and four and more roots (above the curve) for three values of $K(V)$ and the same parameters as in *a*

For constant values of $K(V) \equiv K$ the number of terms in the r.h.s. of (45) does not depend on the volume and, consequently, in thermodynamic limit $V \to \infty$ only the rightmost simple pole in the complex λ plane survives out of a finite number of simple poles. According to the inequality (46), the real root λ_0 is the rightmost singularity of isobaric partition (39). However, there is a possibility that the real parts of other roots $\lambda_{n>0}$ become infinitesimally close to R_0, when there is an infinite number of terms which contribute to the GCP (42).

Let us show now that even for an infinite number of simple poles in (42) only the real root λ_0 survives in the limit $V \to \infty$. For this purpose consider the limit $\mathrm{Re}\,(\nu_n) \gg T$. In this limit the distance between the imaginary parts of the nearest roots remains finite even for infinite volume. Indeed, for $\mathrm{Re}\,(\nu_n) \gg T$ the leading contribution to the r.h.s. of (45) corresponds to the harmonic with $k = K$, and, consequently, an exponentially large amplitude of this term can be only compensated by a vanishing value of $\sin\,(I_n\, bK)$, i.e., $I_n\, bK = \pi n + \delta_n$

with $|\delta_n| \ll \pi$ (hereafter we will analyze only the branch $I_n > 0$), and, therefore, the corresponding decay/formation time $\tau_n \approx K[\pi n T]^{-1}$ is volume independent.

Keeping the leading term on the r.h.s. of (45) and solving for δ_n, one finds

$$I_n \approx (-1)^{n+1} \tilde{\phi}_K(T) \exp\left(\frac{\mathrm{Re}\,(\nu_n)\, K}{T}\right) \delta_n, \tag{47}$$

with

$$\delta_n \approx \frac{(-1)^{n+1}\pi n}{K b\, \tilde{\phi}_K(T)} \exp\left(-\frac{\mathrm{Re}\,(\nu_n)\, K}{T}\right),$$

$$R_n \approx (-1)^n \tilde{\phi}_K(T) \exp\left(\frac{\mathrm{Re}\,(\nu_n)\, K}{T}\right), \tag{48}$$

where in the last step we used Eq. (44) and condition $|\delta_n| \ll \pi$. Since for $V \to \infty$ all negative values of R_n cannot contribute to the GCP (42), it is sufficient to analyze even values of n which, according to (48), generate $R_n > 0$.

Since the inequality (46) cannot be broken, a single possibility, when $\lambda_{n>0}$ pole can contribute to the partition (42), corresponds to the case $R_n \to R_0 - 0^+$ for some finite n. Assuming this, we find $\mathrm{Re}\,(\nu(\lambda_n)) \to \mathrm{Re}\,(\nu(\lambda_0))$ for the same value of μ. Substituting these results into equation (44), one gets

$$R_n \approx \sum_{k=1}^{K} \tilde{\phi}_k(T) \exp\left(\frac{\mathrm{Re}\,(\nu(\lambda_0))\, k}{T}\right) \cos\left[\frac{\pi n k}{K}\right] \ll R_0. \tag{49}$$

The inequality (49) follows from the equation for R_0 and the fact that, even for equal leading terms in the sums above (with $k = K$ and even n), the difference between R_0 and R_n is large due to the next-to-leading term $k = K - 1$, which is proportional to $\exp\left(\dfrac{\mathrm{Re}\,(\nu(\lambda_0))\,(K-1)}{T}\right) \gg 1$. Thus, we arrive at a contradiction with our assumption $R_0 - R_n \to 0^+$, and, consequently, it cannot be true. Therefore, for large volumes the real root λ_0 always gives the main contribution to the GCP (42), and this is the only root that survives in the limit $V \to \infty$. Thus, we showed that the model with the fixed size of the largest fragment has no phase transition because there is a single singularity of the isobaric partition (39), which exists in thermodynamic limit.

8. FINITE VOLUME ANALOGS OF PHASES

If $K(V)$ monotonically grows with the volume, the situation is different. In this case for positive value of $\mathrm{Re}\,(\nu) \gg T$ the leading exponent in the r.h.s. of (45) also corresponds to the largest fragment, i.e., to $k = K(V)$. Therefore, we can apply the same arguments which were used above for the case $K(V) =$

$K = \text{const}$ and derive similarly equations (47), (48) for I_n and R_n. From $I_n \approx \dfrac{\pi n}{b\,K(V)}$ it follows that, when V increases, the number of simple poles in (41) also increases and the imaginary part of the closest to the real λ-axis poles becomes very small, i.e., $I_n \to 0$ for $n \ll K(V)$, and, consequently, the associated decay/formation time $\tau_n \approx K(V)[\pi n T]^{-1}$ grows with the volume of the system. Due to $I_n \to 0$, the inequality (49) cannot be established for the poles with $n \ll K(V)$. Therefore, in contrast to the previous case, for large $K(V)$ the simple poles with $n \ll K(V)$ will be infinitesimally close to the real axis of the complex λ plane.

From Eq. (48) it follows that

$$R_n \approx \frac{p_l(T,\mu)}{T} - \frac{1}{K(V)b}\,\ln\left|\frac{R_n}{\tilde{\phi}_K(T)}\right| \to \frac{p_l(T,\mu)}{T} \tag{50}$$

for $|\mu| \gg T$ and $K(V) \to \infty$. Thus, we proved that for infinite volume the infinite number of simple poles moves toward the real λ axis to the vicinity of liquid phase singularity $\lambda_l = p_l(T,\mu)/T$ of the isobaric partition [19, 20] and generates an essential singularity of function $\mathcal{F}(V, p_l/T)$ in (40) *irrespective of the sign of the chemical potential* μ. In addition, as we showed above, the states with $\mathrm{Re}\,(\nu) \gg T$ become stable because they acquire infinitely large decay/formation time τ_n in the limit $V \to \infty$. Therefore, these states should be identified as a liquid phase for finite volumes as well.

Now it is clear that each curve in the lower panel of Fig. 4, *b* is the finite volume analog of the phase boundary $T - \mu$ for a given value of $K(V)$: below the phase boundary there exists a gaseous phase, but at and above each curve there are states which can be identified with a finite volume analog of the mixed phase, and, finally, at $\mathrm{Re}\,(\nu) \gg T$ there exists a liquid phase. When there is no phase transition, i.e., $K(V) = K = \text{const}$, the structure of simple poles is similar, but, first, the line which separates the gaseous states from the metastable states does not change with the volume, and, second, as is shown above, the metastable states will never become stable. Therefore, a systematic study of the volume dependence of free energy (or pressure for very large V) along with the formation and decay times may be of a crucial importance for experimental studies of the nuclear liquid gas phase transition.

The above results demonstrate that, in contrast to Hill's expectations [9], the finite volume analog of the mixed phase does not consist just of two pure phases. The mixed phase for finite volumes consists of a stable gaseous phase and the set of metastable states which differ by the free energy. Moreover, the difference between the free energies of these states is not surface-like, as Hill assumed in his treatment [9], but volume-like. Furthermore, according to Eqs. (44) and (45), each of these states consists of the same fragments, but with different weights. As is seen from above for the case $\mathrm{Re}\,(\nu) \gg T$, some fragments that belong to the

states, in which the largest fragment is dominant, may, in principle, have negative weights (effective number of degrees of freedom) in the expression for $R_{n>0}$ (44). This can be understood easily because higher concentrations of large fragments can be achieved at the expense of the smaller fragments and is reflected in the corresponding change of the real part of the free energy $-R_{n>0}VT$. Therefore, the actual structure of the mixed phase at finite volumes is more complicated than was expected in earlier works.

The Hills ideas were developed further in [8], where the authors claimed to establish the one-to-one correspondence between the bimodal structure of the partition of measurable quantity B known on average and the properties of the Lee–Yang zeros of this partition in the complex g plane. The starting point of [8] is to postulate the partition Z_g and the probability $P_g(B)$ of the following form:

$$Z_g \equiv \int dB\, W(B)\, \mathrm{e}^{-Bg} \Rightarrow P_g(B) \equiv \frac{W(B)\, \mathrm{e}^{-Bg}}{Z_g}, \tag{51}$$

where $W(B)$ is the partition sum of the ensemble of fixed values of the observable $\{B\}$, and g is the corresponding Lagrange multiplier. Then the authors of [8] assume the existence of two maxima of the probability $P_g(B)$ ($\equiv$ bimodality) and discuss their relation to the Lee–Yang zeros of Z_g in the complex g plane.

The CSMM gives us a unique opportunity to verify the Chomaz and Gulminelli idea on the bimodality behavior of $P_g(B)$ using the first principle results. Let us use Eq. (38) identifying the intensive variable g with λ and extensive one B with the available volume $V' \to \tilde{V}$. The evaluation of the r.h.s. of (38) is very difficult in general, but for a special case, when the eigen volume b is small this can be done analytically. Thus, approximating $\mathcal{F}(\xi, \lambda - i\eta) \approx \mathcal{F}(\xi, \lambda) - i\eta \partial \mathcal{F}(\xi, \lambda)/\partial\lambda$, we obtain the CSMM analog of the probability (51)

$$P_\lambda(\tilde{V})\hat{\mathcal{Z}}(\lambda, T, \mu) \equiv \int\limits_{-\infty}^{+\infty} d\xi \int\limits_{-\infty}^{+\infty} \frac{d\eta}{2\pi}\, \mathrm{e}^{i\eta(\tilde{V}-\xi)-\lambda\tilde{V}+\tilde{V}\mathcal{F}(\xi,\lambda-i\eta)} \approx$$

$$\approx \int\limits_{-\infty}^{+\infty} d\xi\, \mathrm{e}^{\tilde{V}[\mathcal{F}(\xi,\lambda)-\lambda]} \delta\left[\tilde{V} - \xi - \frac{\partial \mathcal{F}(\xi, \lambda)}{\partial\lambda}\right], \tag{52}$$

where we made the η integration after applying the approximation for $\mathcal{F}(\xi, \lambda - i\eta)$. Further evaluation of (52) requires to know all possible solutions of the average volume of the system $\xi^*_\alpha(\tilde{V}) = \tilde{V} - \partial\mathcal{F}(\xi^*_\alpha, \lambda)/\partial\lambda$ ($\alpha = \{1, 2, \dots\}$). It can be shown [50] that for the gaseous domain $\nu = \mathrm{Re}\,(\nu) < -2T$ (see Fig. 4, *b*) there exists a single solution $\alpha = 1$, whereas for the domain $\nu = \mathrm{Re}\,(\nu) > 0$, which corresponds to a finite volume analog of the mixed phase, there are two solutions

$\alpha = 1, 2$. In contrast to the expectations of [8], the probability (52)

$$P_\lambda(\tilde{V})\ \hat{\mathcal{Z}}(\lambda, T, \mu) \approx$$
$$\approx \sum_\alpha \frac{1}{\left|1 + \dfrac{\partial^2 \mathcal{F}(\xi^*_\alpha, \lambda)}{\partial \lambda \xi^*_\alpha}\right|} \mathrm{e}^{\tilde{V}[\mathcal{F}(\xi,\lambda)-\lambda]} \Rightarrow \frac{\partial \ln P_\lambda(\tilde{V})}{\partial \tilde{V}} \leqslant 0 \quad (53)$$

has negative derivative for the whole domain of existence of the isobaric partition $\hat{\mathcal{Z}}(\lambda, T, \mu)$ [50]. This is true even for the domain in which, as we proved, there exists a finite analog of the mixed phase, i.e., for $\nu = \mathrm{Re}\,(\nu) > 0$. Moreover, irrespective of the sign of the derivative $\dfrac{\partial \ln P_\lambda(\tilde{V})}{\partial \tilde{V}}$, the probability (52) cannot be measured experimentally. Above it was rigorously proven that for any real ξ the IP $\hat{\mathcal{Z}}(\lambda, T, \mu)$ is defined on the real λ axis only for $\mathcal{F}(\xi, \lambda) - \lambda > 0$, i.e., on the right-hand side of the gaseous singularity λ_0: $\lambda > \lambda_0$. However, as one can see from equation (41), the «experimental» λ_n values belong to the other region of the complex λ plane: $\mathrm{Re}\,(\lambda_{n>0}) < \lambda_0$.

Thus, it turns out that the suggestion of [8] to analyze the probability (51) does not make any sense because, as we showed explicitly for the CSMM, it cannot be measured. It seems that the starting point of the [8] approach, i.e., the assumption that the left equation (51) gives the most general form of the partition of finite system, is problematic. Indeed, comparing (50) with the analytical result (53), we see that for finite systems, in contrast to the major assumption of [8], the probability W of the CSMM depends not only on the extensive variable $\tilde{V}$, but also on the intensive variable λ, which makes unmeasurable the whole construct of [8]. Consequently, the conclusions of [8] on the relation between the bimodality and the phase transition existence are not general and have a limited range of validity. In addition, the absence of two maxima of the probability (53) automatically means the absence of back-banding of the equation of state [8].

9. GAS OF BAGS IN FINITE VOLUMES

Now we will apply the formalism of the preceding sections to the analysis of the Gas of Bags Model (GBM) [36, 52] in finite volumes. In the low and high temperature domains the GBM reduces to two well-known and successful models: the hadron gas model [53] and the bag model of QGP [54]. Both of these models are surprisingly successful in describing the bulk properties of hadron production in high energy nuclear collisions, and, therefore, one may hope that their generalization, the GBM, may reflect basic features of the nature in the phase transition region.

The Van der Waals gas consisting of n hadronic species, which are called bags in what follows, has the following GCP [36]:

$$Z(V,T) = \sum_{\{N_k\}} \left[\prod_{k=1}^{n} \frac{\left[(V - v_1 N_1 - \ldots - v_n N_n)\, \phi_k(T) \right]^{N_k}}{N_k!} \right] \times \\ \times\, \theta(V - v_1 N_1 - \ldots - v_n N_n), \quad (54)$$

where $\phi_k(T) \equiv g_k \phi(T, m_k) \equiv \dfrac{g_k}{2\pi^2} \int\limits_0^\infty p^2 dp \, \exp\left[-\dfrac{(p^2 + m_k^2)^{1/2}}{T} \right] = g_k \dfrac{m_k^2 T}{2\pi^2} \times$ $K_2\left(\dfrac{m_k}{T}\right)$ is the particle density of bags of mass m_k, eigen volume v_k and degeneracy g_k. This expression differs slightly form the GCP of the simplified SMM (3), where $\mu = 0$ and the eigen volume of k-nucleon fragment kb is changed to the eigen volume of the bag v_k. Therefore, as for the simplified SMM the Laplace transformation (4) with respect to volume of Eq. (54) gives

$$\hat{Z}(s,T) = \left[\, s - \sum_{j=1}^{n} \exp\left(-v_j s\right) g_j \phi(T, m_j) \right]^{-1}. \quad (55)$$

In preceding sections we showed that as long as the number of bags, n, is finite, the only possible singularities of $\hat{Z}(s,T)$ (55) are simple poles. However, in the case of an infinite number of bags an essential singularity of $\hat{Z}(s,T)$ may appear. This property is used in the GBM: the sum over different bag states in (54) can be replaced by the integral, $\sum\limits_{j=1}^{\infty} g_j \ldots = \int\limits_0^\infty dm\, dv \ldots \rho(m,v)$, if the bag mass-volume spectrum, $\rho(m,v)$, which defines the number of bag states in the mass-volume region $[m, v; m+dm, v+dv]$, is given. Then, the Laplace transform of $Z(V,T)$ reads [36]

$$I\hat{Z}_{\rm GB}(s,T) \equiv \int\limits_0^\infty dV \, \mathrm{e}^{-sV} \, Z(V,T) = \left[s - f(T,s) \right]^{-1}, \\ \text{where} \qquad f(T,s) = \int\limits_0^\infty dm\, dv \rho(m,v)\, \mathrm{e}^{-vs} \phi(T,m). \quad (56)$$

Like in the simplified SMM, the pressure of infinite system is again given by the rightmost singularity: $p(T) = T s^*(T) = T \cdot \max\left\{ s_H(T), s_Q(T) \right\}$. Similarly to the simplified SMM considered in Secs. 2 and 3, the rightmost singularity $s^*(T)$

of $\hat{Z}(s,T)$ (56) can be either the simple pole singularity $s_H(T) = f(T, s_H(T))$ of the isobaric partition (56) or the $s_Q(T)$ singularity of the function $f(T,s)$ (56) itself.

The major mathematical difference between the simplified SMM and the GBM is that the latter employs the two-parameter mass-volume spectrum. Thus, the mass-volume spectrum of the GBM consists of the discrete mass-volume spectrum of light hadrons and the continuum contribution of heavy resonances [55]

$$\rho(m,v) = \sum_{j=1}^{J_m} g_j \delta(m-m_j)\ \delta(v-v_j) + \Theta(v-V_0)\Theta(m-M_0-Bv)\times \\ \times Cv^{\gamma}(m-Bv)^{\delta}\ \exp\left[\frac{4}{3}\sigma_Q^{1/4}v^{1/4}(m-Bv)^{3/4}\right], \quad (57)$$

respectively. Here $m_j < M_0$, $v_j < V_0$, $M_0 \approx 2$ GeV, $V_0 \approx 1$ fm^3, C, γ, δ, and B (the so-called bag constant, $B \approx 400$ MeV/fm^3) are the model parameters and

$$\sigma_Q = \frac{\pi^2}{30}\left(g_g + \frac{7}{8}g_{q\bar{q}}\right) = \frac{\pi^2}{30}\left(2\cdot 8 + \frac{7}{8}\cdot 2\cdot 2\cdot 3\cdot 3\right) = \frac{\pi^2}{30}\ \frac{95}{2} \quad (58)$$

is the Stefan–Boltzmann constant counting gluons (spin, color) and (anti)quarks (spin, color and u, d, s flavor) degrees of freedom.

Recently the grand canonical ensemble has been heavily criticized [56, 57], when it is used for the exponential mass spectrum. This critique, however, cannot be applied to the mass-volume spectrum (57) because it grows less fast than the Hagedorn mass spectrum discussed in [56, 57], and because in the GBM there is an additional suppression of large and heavy bags due to the Van der Waals repulsion. Therefore, the spectrum (57) can be safely used in the grand canonical ensemble.

It can be shown [52] that the spectrum (57) generates the $s_Q(T) = \dfrac{\sigma_Q}{3}T^3 - \dfrac{B}{T}$ singularity, which reproduces the bag model pressure $p(T) = Ts_Q(T)$ [54] for high temperature phase, and $s_H(T)$ singularity, which gives the pressure of the hadron gas model [53] for low temperature phase. The transition between them can be of the first order or second order or cross-over, depending on the model parameters.

However, for finite systems the volume of bags and their masses should be finite. The simplest finite volume modification of the GBM is to introduce the volume-dependent size of the largest bag $n = n(V)$ in the partition (54). As we discussed earlier such a modification cannot be handled by the traditional Laplace transform technique used in [52,55], but this modification can be easily accounted for by the Laplace–Fourier method [32]. Repeating all the steps of Secs. 5 and 6, we shall obtain the equations (40)–(43), in which the function $\mathcal{F}(\xi, \tilde{\lambda})$ should

be replaced by its GBM analog $f(\lambda, V_B) \equiv f_H(\lambda) + f_Q(\lambda, V_B)$ defined via

$$f_H(\lambda) \equiv \sum_{j=1}^{J_m} g_j \phi(T, m_j)\, \mathrm{e}^{-v_j s},$$

and

$$f_Q(\lambda, V_B) \equiv V_0 \int\limits_1^{V_B/V_0} dk a(T, V_0 k)\, \mathrm{e}^{V_0(s_Q(T)-\lambda)k}. \tag{59}$$

In evaluating (59) we used the mass-volume spectrum (57) with the maximal volume of the bag V_B and changed integration to a dimensionless variable $k = v/V_0$. Here the function $a(T, v) = u(T)v^{2+\gamma+\delta}$ is defined by $u(T) = C\pi^{-1}\sigma_Q^{\delta+1/2}T^{4+4\delta}(\sigma_Q T^4 + B)^{3/4}$.

The above representation (59) generates equations for the real and imaginary parts of $\lambda_n \equiv R_n + iI_n$, which are very similar to the corresponding expressions of the CSMM (44) and (45). Comparing (59) with (43), one sees that their main difference is that the sum over k in (43) is replaced by the integral over k in (59). Therefore, equations (44) and (45) remain valid for R_n and I_n of the GBM, respectively if we replace the k sum by the integral for $K(V) = V_B/V_0$, $b = V_0$, $\nu(\lambda) = V_0(s_Q(T) - \lambda)$, and $\tilde{\phi}_{k>1}(T) = V_0 a(T, V_0 k)$. Thus, the results and conclusions of our analysis of the R_n and I_n properties of the CSMM should be valid for the GBM as well. In particular, for large values of $K(V) = V_B/V_0$ and $R_n < s_Q(T)$, one can immediately find out $I_n \approx \pi n/V_B$ and the GBM formation/decay time $\tau_n = V_B[\pi n T V_0]^{-1}$. These equations show that the metastable $\lambda_{n>0}$ states can become stable in thermodynamic limit if and only if $V_B \sim V$.

The finite volume modification of the GBM equation of state should be used for the quantities which have $V\lambda_0 \sim 1$. This may be important for the early stage of the relativistic nuclear collisons when the volume of the system is small, or for the systems that have small pressures. The latter can be the case for the pressure of strange or charm hadrons.

10. HILLS AND DALES MODEL AND THE SOURCE OF SURFACE ENTROPY

During last forty years the Fisher droplet model (FDM) [22] has been successfully used to analyze the condensation of a gaseous phase (droplets or clusters of all sizes) into a liquid. The systems analyzed with the FDM are many and varied, but up to now the source of the surface entropy is not absolutely clear. In his original work Fisher postulated that the surface free-energy F_A of a cluster of A constituents consists of surface ($A^{2/3}$) and logarithmic ($\ln A$) parts, i.e.,

$F_A = \sigma(T)A^{2/3} + \tau T \ln A$. Its surface part $\sigma(T)A^{2/3} \equiv \sigma_0[1 - T/T_c]A^{2/3}$ consists of the surface energy, i.e., $\sigma_0 A^{2/3}$, and surface entropy $-\sigma_0/T_c A^{2/3}$. From the study of the combinatorics of lattice gas clusters in two dimensions, Fisher postulated the specific temperature dependence of the surface tension $\sigma(T)|_{\rm FDM}$ which gives naturally an estimate for the critical temperature T_c. Surprisingly Fisher's estimate works for the 3D Ising model [58], nucleation of real fluids [59, 60], percolation clusters [61] and nuclear multifragmentation [3].

To understand why the surface entropy has such a form we formulated a statistical model of surface deformations of the cluster of A constituents, the Hills and Dales Model (HDM) [33]. For simplicity we consider cylindrical deformations of positive height $h_k > 0$ (hills) and negative height $-h_k$ (dales), with k constituents at the base. It is assumed that cylindrical deformations of positive height $h_k > 0$ (hills) and negative height $-h_k$ (dales), with k constituents at the base, and the top (bottom) of the hill (dale) has the same shape as the surface of the original cluster of A constituents. We also assume that: (i) the statistical weight of deformations $\exp\left(-\sigma_0|\Delta S_k|/s_1/T\right)$ is given by the Boltzmann factor due to the change of the surface $|\Delta S_k|$ in units of the surface per constituent s_1; (ii) all hills of heights $h_k \leqslant H_k$ (H_k is the maximal height of a hill with a base of k constituents) have the same probability dh_k/H_k besides the statistical one; (iii) assumptions (i) and (ii) are valid for the dales.

The HDM grand canonical surface partition (GCSP)

$$Z_{\rm gc}(S_A) = \sum_{\{n_k^{\pm}=0\}}^{\infty} \left[\prod_{k=1}^{K_{\max}} \frac{\left[z_k^+ \mathcal{G}_{\rm gc}\right]^{n_k^+}}{n_k^+!} \frac{\left[z_k^- \mathcal{G}_{\rm gc}\right]^{n_k^-}}{n_k^-!} \right] \Theta(s_1 \mathcal{G}_{\rm gc}) \tag{60}$$

corresponds to the conserved (on average) volume of the cluster because the probabilities of hill z_k^+ and dale z_k^- of the same k-constituent base are identical [33]

$$z_k^{\pm} \equiv \int_0^{\pm H_k} \frac{dh_k}{\pm H_k} \exp\left(-\frac{\sigma_0 P_k |h_k|}{T s_1}\right) = \frac{T s_1}{\sigma_0 P_k H_k} \left[1 - \exp\left(-\frac{\sigma_0 P_k H_k}{T s_1}\right)\right]. \tag{61}$$

Here P_k is the perimeter of the cylinder base.

The geometrical partition (degeneracy factor) of the HDM or the number of ways to place the center of a given deformation on the surface of the A-constituent cluster which is occupied by the set of $\{n_l^{\pm} = 0, 1, 2, \ldots\}$ deformations of the l-constituent base are assumed to be given in the Van der Waals approximation [33]:

$$\mathcal{G}_{\rm gc} = \left[S_A - \sum_{k=1}^{K_{\max}} k(n_k^+ + n_k^-) s_1 \right] s_1^{-1}, \tag{62}$$

where $s_1 k$ is the area occupied by the deformation of k-constituent base ($k = 1, 2, \ldots$); S_A is the full surface of the cluster, and $K_{\max}(S_A)$ is the A-dependent size of the maximal allowed base on the cluster.

The $\Theta(s_1 \mathcal{G}_{\rm gc})$ function in (1) ensures that only configurations with positive value of the free surface of cluster are taken into account, but makes the analytical evaluation of the GCSP (1) very difficult. However, we were able *to solve this GCSP exactly* for any surface dependence of $K_{\max}(S_A)$ using identity (37) of the Laplace–Fourier transform technique [32]:

$$Z_{\rm gc}(S_A) = \sum_{\{\lambda_n\}} {\rm e}^{\lambda_n S_A} \left[1 - \frac{\partial \mathcal{F}_{\rm gc}(S_A, \lambda_n)}{\partial \lambda_n} \right]^{-1}. \tag{63}$$

The poles λ_n of the isochoric partition are defined by

$$\lambda_n = \mathcal{F}_{\rm gc}(S_A, \lambda_n) \equiv \sum_{k=1}^{K_{\max}(S_A)} \left[\frac{z_k^+}{s_1} + \frac{z_k^-}{s_1} \right] {\rm e}^{-k\, s_1 \lambda_n}. \tag{64}$$

Our analysis shows that Eq. (5) has exactly one real root $R_0^{\rm gc} = \lambda_0$, ${\rm Im}\,(\lambda_0) = 0$, which is the rightmost singularity, i.e., $R_0^{\rm gc} > {\rm Re}\,(\lambda_{n>0})$. As proved in [33], the real root $R_0^{\rm gc}$ dominates completely for clusters with $A \geqslant 10$.

Also we showed that there is an absolute supremum for the real root $R_0^{\rm gc}$, which corresponds to the limit of infinitesimally small amplitudes of deformations, $H_k \to 0$, of large clusters: $\omega^{\rm gc} \equiv \sup(R_0^{\rm gc}) = 1.06009 \equiv R_0^{\rm gc} = 2 \left[{\rm e}^{R_0^{\rm gc}} - 1 \right]^{-1}$. It is remarkable that the last result is, first, model independent because in the limit of vanishing amplitude of deformations all model specific parameters vanish; and, second, it is valid for any self-nonintersecting surfaces.

For large spherical clusters the GCSP becomes $Z(S_A) \approx 0.3814\, {\rm e}^{1.06009\, A^{2/3}}$, which, combined with the Boltzmann factor of the surface energy ${\rm e}^{-\sigma_0 A^{2/3}/T}$, generates the following temperature-dependent surface tension of the large cluster $\sigma(T) = \sigma_0 \left[1 - 1.06009 \dfrac{T}{\sigma_0} \right]$. This result means that the actual critical temperature of the FDM should be $T_c = \sigma_0 / 1.06009$, i.e., 6.009% smaller in σ_0 units than Fisher originally supposed.

Similarly one can introduce the surface partitions for the other ensembles [34]. The canonically constrained surface partition (CCSP) is built up to obey the volume conservation more strictly than it is done in the GCSP. This is ensemble of pairs of deformations: the number of the hills n_k^+ of the k-constituent base is always identical to the number of corresponding dales, i.e., $n_k^- \equiv n_k^+ \equiv n_k$. Then the canonical geometrical partition can be cast as

$$\mathcal{G}_c = \left[S_A - 2 \sum_{k=1}^{K_{\max}} k n_k s_1 \right] (2 s_1)^{-1}, \tag{65}$$

where the factor two in the denominator of the right-hand side (r.h.s.) of (65) accounts for the fact that it is necessary to place simultaneously the centers of two k-constituent base deformations (hill and dale) out of $2n_k$ on the surface of cluster. Using the geometrical partition (65), one can obtain the partition function of canonical ensemble by formally replacing $\mathcal{G}_{\rm gc} \to \mathcal{G}_c$ and inserting the Kronecker $\delta_{n_k^+,n_k^-}$ for each k multiplier in (60). We, however, consider each pair of hills and dales of the same base as a single degree of freedom. Therefore, the number of ways to place each pair out of n_k distinguishable pairs is still given by the canonical geometrical partition $\mathcal{G}_c$. Multiplying it with the probability of a pair of deformations $z_k^+ z_k^-$ and repeating this for n_k pairs, we obtain the CCSP as follows:

$$Z_{\rm cc}(S_A) = \sum_{\{n_k=0\}}^{\infty} \left[\prod_{k=1}^{K_{\max}} \frac{\left[z_k^+ z_k^- \mathcal{G}_c\right]^{n_k}}{n_k!} \right] \Theta(2 s_1 \mathcal{G}_c). \tag{66}$$

Applying the Laplace–Fourier transform technique to this partition, one can find that the CCSP has the same form as the GCSP (63), but the function $\mathcal{F}_{\rm gc}$ in (64) must be replaced with $\mathcal{F}_{\rm cc}$:

$$\lambda_n = \mathcal{F}_{\rm cc}(S_A, \lambda_n) = \sum_{k=1}^{K_{\max}(S_A)} \frac{z_k^+ z_k^-}{2\, s_1} \, \mathrm{e}^{-2k s_1 \lambda_n}. \tag{67}$$

For the limit of the vanishing amplitudes of deformations it is possible to introduce one more ensemble for the surface deformations [34] which hereafter will be called as the *semigrand canonical surface partition* (SGCSP). This ensemble occupies an intermediate position between the constrained canonical and grand canonical formulations. It corresponds to the case, when the hills and dales of the same base are considered to be indistinguishable. For that we would like to explore the fact that according to (61) the statistical probabilities of hills and dales of the same base are equal. Then for the infinitesimally small amplitudes of deformations the volume conservation constraint is fulfilled trivially. In the present work this ensemble will be used for the deformations of vanishing amplitude only, but it may be used also for finite amplitudes of deformations if the volume is not conserved. Then the SGCSP and its geometrical factor read as

$$\begin{aligned} Z_{\rm sg}(S_A) &= \sum_{\{n_k=0\}}^{\infty} \left[\prod_{k=1}^{K_{\max}} \frac{\left[z_k^+ \mathcal{G}_{\rm sg}\right]^{n_k}}{n_k!} \right] \Theta(s_1 \mathcal{G}_{\rm sg}), \\ \mathcal{G}_{\rm sg} &= \left[S_A - \sum_{k=1}^{K_{\max}} k n_k s_1 \right] s_1^{-1}. \end{aligned} \tag{68}$$

Again, like in the case of the CCSP, only the equation for the simple poles of the isochoric partition should be modified

$$\lambda_n = \mathcal{F}_{\rm sg}(S_A, \lambda_n) = \sum_{k=1}^{K_{\max}(S_A)} \frac{z_k^+}{s_1}\, {\rm e}^{-k s_1 \lambda_n}. \tag{69}$$

It can be shown that for all surface partitions discussed in this section the properties of singularities λ_n of the isochoric partitions are the same [34]. There is only a quantitative difference for the rightmost singularities $R_0^\alpha \equiv s_1 L^\alpha \lambda_0^\alpha$ ($\alpha \in \{{\rm gc}, {\rm sg}, {\rm cc}\}$), where L^α are defined as $L^{\rm gc} = L^{\rm sg} = 1$ and $L^{\rm cc} = 2$. Therefore, in the limit of the vanishing amplitudes of deformations for an infinite base of the largest deformation $K_{\max}(S_A \to \infty) \to \infty$ each of these surface partitions will reach an *upper limit* defined by the corresponding value of the surface entropy coefficient ω_U^α

$$\begin{gathered} \max\{Z_\alpha(S_A)\} \to g_\alpha \exp\left(\omega_U^\alpha \frac{S_A}{s_1}\right) \\ \text{with} \quad \omega_U^\alpha = \begin{cases} \omega_U^{\rm gc} = \max\{R_0^{\rm gc}\} \approx 1.060090, & \alpha = {\rm gc}, \\ \omega_U^{\rm cc} = \max\{R_0^{\rm cc}/2\} \approx 0.403233, & \alpha = {\rm cc}, \\ \omega_U^{\rm sg} = \max\{R_0^{\rm sg}\} \approx 0.806466, & \alpha = {\rm sg}, \end{cases} \end{gathered} \tag{70}$$

where the degeneracy factor g_α is defined as follows: $g_{\rm gc} \approx 0.38139$ and $g_{\rm cc} = g_{\rm sg} \approx 0.407025$.

For large, but finite clusters it is necessary to take into account not only the rightmost singularity λ_0^α of the corresponding surface partition, but all other singularities $\lambda_{n>0}^\alpha$ with positive real part $R_{n>0}^\alpha > 0$. However, the analysis presented in [34] shows that for the clusters of a few constituents the rightmost singularity of the isochoric partition completely dominates. This can be seen in Fig. 5, which depicts a few roots λ_n^α for the vanishing amplitudes of deformations.

The obtained surface tension coefficients can be compared with the corresponding value of the ω-coefficient of the d-dimensional Ising model. The latter is defined as the energy $2J$ required to flip a given spin interacting with its q neighbors to opposite direction per $(d-1)$-dimensional surface divided by the value of critical temperature

$$\omega_{\rm Lat} = \frac{qJ}{T_{\rm c} d}. \tag{71}$$

Here q is the coordination number for the lattice, and J denotes the coupling constant of the model. A comparison of ω_U^α values in (70) with Tables 1 and 3 shows that all lattice $\omega_{\rm lat}$-coefficients, indeed, lie between the upper estimates for

the constrained canonical and grand canonical surface partitions

$$0.403233 = \omega_U^{\rm cc} < \omega_{\rm lat} < \omega_U^{\rm gc} = 1.060090, \tag{72}$$

i.e., $\omega_U^{\rm cc}$ and $\omega_U^{\rm gc}$ are the infimum and supremum for 2- and 3-dimensional Ising models, respectively.

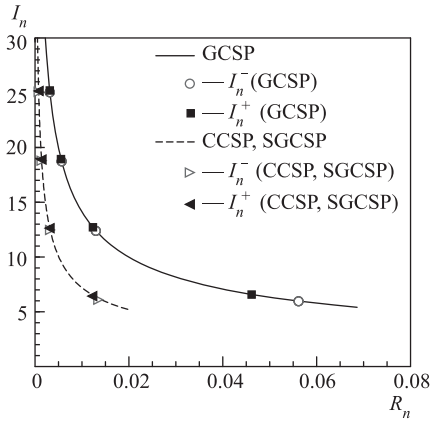

Fig. 5. The first quadrant of the complex plane $(R_n^\alpha + iI_n^\alpha) \equiv s_1\lambda_n^\alpha L^\alpha$ shows the location of simple poles of the isochoric partitions for $n = 1, 2, 3, 4$. The symbols represent the two branches I_n^- and I_n^+ of the roots for the upper estimate of three surface partitions. The curves are defined by the approximation suggested in [34]

Table 2. **The values of the $\omega_{\rm lat}$ coefficient for various 2-dimensional Ising models. For more details see the text**

Lattice type	$\omega_{\rm lat} = \sigma/T_c$
Honeycomb	0.987718
Kagome	0.933132
Square	0.881374
Triangular	0.823960
Diamond	0.739640

Table 3. **The values of the $\omega_{\rm lat}$ coefficient for various 3-dimensional Ising models**

Lattice type	$\omega_{\rm lat} = \sigma/T_c$
Simple cubic	0.44342
Body-centered cubic	0.41989
Face-centered cubic	0.40840

It is remarkable that such a simple model of surface partition discussed above gives the upper and lower bounds of ω coefficients for all 2- and 3-dimensional Ising models. While further intriguing facts can be found in the original work [34], here we mention only that the surface tension plays a very important role in the SMM and CSMM, but its influence on the properties of the phase diagram of the GBM is not understood yet. Another interesting problem of surface partition is to consider the fractal deformations within the HDM in order to elucidate the source of Fisher's power law. We believe that these problems are of great importance.

11. STRATEGY OF SUCCESS

Here we discuss exact analytical solutions of a variety of statistical models which are obtained by a new powerful mathematical method, the Laplace–Fourier transform. Using this method we solved the constrained SMM and Gas of Bags Model for finite volumes, and found the surface partition of large clusters. Since in the thermodynamic limit the CSMM has the nuclear liquid–gas PT and the GBM describes the PT between the hadron gas and QGP, it was interesting and important to study them for finite volumes. As we have shown, for finite volumes their GCP functions can be identically rewritten in terms of the simple poles $\lambda_{n\geqslant 0}$ of the isobaric partition (39). We proved that the real pole λ_0 exists always and the quantity $T\lambda_0$ is the constrained grand canonical pressure of the gaseous phase. The complex roots $\lambda_{n>0}$ appear as pairs of complex conjugate solutions of equation (43). Their most straightforward interpretation is as follows: $-T\,\mathrm{Re}\,(\lambda_n)$ has a meaning of the free energy density, whereas $bT\,\mathrm{Im}\,(\lambda_n)$, depending on its sign, gives the inverse decay/formation time of such a state. Therefore, the gaseous state is always stable because its decay/formation time is infinite and because it has the smallest value of free energy, whereas the complex poles describe the metastable states for $\mathrm{Re}\,(\lambda_{n>0}) \geqslant 0$ and mechanically unstable states for $\mathrm{Re}\,(\lambda_{n>0}) < 0$.

We studied the volume dependence of the simple poles and found a dramatic difference in their behavior for the case with phase transition and without it. For the case with phase transition this formalism allows one to define the finite volume analogs of phases unambiguously and to establish the finite volume analog of the $T-\mu$ phase diagram (see Fig. 4). At finite volumes the gaseous phase is described by a simple pole λ_0, the mixed phase corresponds to a finite number of simple poles (three and more), whereas the liquid is represented by an infinite amount of simple poles at $|\mu| \to \infty$ which describe the states of a highest possible particle density.

As we showed for the CSMM and GBM, at finite volumes the λ_n states of the same partition with given T and μ are not in a true chemical equilibrium because the interaction between the constituents generates complex values of the effective chemical potential. This feature cannot be obtained within the Fisher droplet model due to the lack of the hard core repulsion between the constituents. We showed that, in contrast to Hill's expectations [9], the mixed phase at finite volumes is not just a composition of two states which are the pure phases. As was shown, a finite volume analog of the mixed phase is a superposition of three and more collective states, and each of them is characterized by its own value of λ_n, and, consequently, the difference between the free energies of these states is not a surface-like, as Hill argued [9], but volume-like.

Also the exact analytical formulas gave us a unique opportunity to verify the Chomaz and Gulminelli ideas [8] about the connection between bimodality and the

phase transition existence for finite volumes. The CSMM exact analytical solution not only provided us with a counterexample for which there is no bimodality in case of finite volume phase transition, but it gave us an explicit example to illustrate that the probability which, according to [8] is supposed to signal the bimodal behavior of the system, cannot be measured experimentally.

All this clearly demonstrates that the exactly solvable models are very useful theoretical tools and they open the new possibilities to study the critical phenomena at finite volumes rigorously. The *short range perspectives (SRP)* of this direction of research are evident:

1. *Study* the isobaric ensemble and the excluded volume correction for the clusters of the 2- and 3-dimensional Ising models, and find out the reliable signals of phase transition on finite lattices.

2. *Widen or refine* the CSMM, GMB, and HDM analytical solutions for more realistic interaction between the constituents. In particular, a more realistic Coulomb interaction between nuclear fragments (not the Wigner–Seitz one!) can be readily included now into the CSMM and may be studied rigorously without taking thermodynamic limit. Also the relativistic Lorentz contraction of the hadronic and bag eigen volumes discussed recently in [62, 63] for a single hadronic specie should be accounted for and studied in the GBM for the temperatures above these of cross-over to QGP. The HDM has to be formulated for fractal deformations, that, hopefully, will shed light on the source of Fisher's power law.

3. *Deepen or extend* the CSMM and GMB models to the canonical and microcanonical formulations, and work out the reliable signals of the finite system phase transitions for this class of models.

The major goals for the SRP are (I) to get the reliable experimental signals obtained not with the *ad hoc* theoretical constructs which are very popular nowadays, but directly from the first principles of statistical mechanics; (II) to work out a common and useful theoretical language for a few nuclear physics communities.

However, even the present (very limited!) amount of exact results can be used as a good starting point to build up a truly microscopic theory of phase transitions in finite systems. In fact, the exact analytical solution, which we found for finite volumes, is one of the key elements that are necessary to create a microscopic kinetics of PTs in finite systems. The formulation of such a theory for nuclear physics is demanded by the reality of the experimental measurements: both of the phase transitions which are studied in nuclear laboratories, the liquid–gas and hadron gas–QGP, are accessible only via the violent nuclear collisions. As a result, in these collisions we are dealing with the PTs which occur not only in finite system, but in addition these PTs happen dynamically. It is known that during the course of collision the system experiences a complicated evolution from a highly excited (on the ordinary level) state which is far from local equilibrium,

to the collective expansion of the locally thermalized state and to a (nearly) free-streaming stage of corresponding constituents.

A tremendous complexity of the nuclear collision process makes it extremely difficult for theoretical modeling. This is, in part, one of the reasons why, despite a great amount of experimental data collected during last 25 years and numerous theoretical attempts, neither the liquid–gas nor the hadron gas–QGP phase transitions are well established experimentally and well understood theoretically. It turns out that the major problem of modeling both of these PTs in dynamic situations is the absence of the suitable theoretical apparatus.

For example, it is widely believed in the Relativistic Heavy Ion community (RHIc) that relativistic hydrodynamics is the best theoretical tool to model the PT between QGP and hadron gas because it employs only the equilibrium equation of state [64]. Up to now this is just a wishful illusion because besides the incorrect boundary conditions, known as «*freeze-out procedure*» [65, 66], which are typically used in the actual hydro calculations [64], the employed equation of state does not fit into the finite (and sometimes small!) size of the system because it corresponds to an infinite system. On the other hand, it is known [67] that hydrodynamic description is limited by the weak (small) gradients of the hydro variables, which define a characteristic scale not only for collective hydro properties, but also a typical volume for the equation of state.

Above we showed that for finite systems the equation of state inevitably includes the volume dependence of such thermodynamic variables as pressure and energy density which are directly involved into hydrodynamic equations. This simple fact is not realized yet in the RHIc, but, probably, the chemical nonequilibrium (which is usually implemented into equation of state by hand) is, in part, generated by the finite volume corrections of the GCP. If this is the case, then, according to our analysis of the finite volume GCP functions, it is necessary to insert the complex values of the chemical potential into hydro calculations.

Unfortunately, at present there is no safe recipe on how to include the finite volume equation of state in the hydrodynamic description. A partial success of the hybrid hydro-cascade models [68, 69], which might be considered as a good alternative to hydrodynamics, is compensated by the fact that none of the existing hydro-cascade models was able to resolve the so-called *HBT puzzles* [16] found in the energy range of the Relativistic Heavy Ion Collider. Moreover, despite the rigorous derivation [70, 71] of the hydro-cascade equations, the hydrodynamic part of this approach is suffering the very same problems of the infinite matter equation of state which we discussed above. Therefore, further refinements of the hydro-cascade models will not be able to lift up the theoretical apparatus of modeling the dynamics of the finite volume PTs to new heights, and we have to search for a more elaborate approach.

It turns out that the recently derived finite domain kinetic equations [70, 71] can provide us with another starting point to develop the first principle microscopic

theory of the critical phenomena in finite systems. These equations generalize the relativistic Boltzmann equation to finite domains and, on the one hand, allow one to conjugate two (different!) kinetics which exist in two domains separated by the evolving boundary, and, on the other hand, to account exactly for the exchange of particles between these domains. (For instance, one can easily imagine the situation when on one side of the boundary separating the domains there may exist one phase of the system which interacts with the other phase located on the other side of the boundary.) But, first, the finite domain kinetic equations should be generalized to the two-particle distribution functions and then they should be adapted to the framework of nuclear multifragmentation and the Gas of Bags Model. In doing this, the exact analytical results we discussed will be indispensable because they provide us with the equilibrium state of the finite system and tell us to what finite volume analog of phases this state belongs.

Therefore, a future success in building up a microscopic kinetics of PTs in finite systems can be achieved if we combine the exact results obtained for equilibrated finite systems with the rigorous kinetic equations suited for finite systems. There is a good chance for the nuclear multifragmentation community to play a very special role in the development of such a theory, namely it may *act as a perfect and reliable test site* to work out and verify the whole concept. This is so because besides some theoretical advances and experience in studying the PTs in finite systems, the experiments at intermediate energies, compared to the searches for QGP, are easier and cheaper to perform, and the PT signals are cleaner and unspoiled by a strong flow. Moreover, once the concept is developed and verified, it can be modified and applied to study other PTs in finite systems, including the transitions to/from high temperature QCD and dense hadronic matter planned to be studied at CERN LHC, at GSI FAIR and, hopefully, at JINR Nuclotron. Thus, after some readjustment, the manpower and experimental facilities of nuclear multifragmentation community can be used for *a new strategic aim,* which is at the frontier line of modern physics.

Such a programme, however, requires the coherent efforts of, at least, two strong and competing theoretical groups, an access to the collected experimental data and an advanced computer facility. Organizationally it will require a very close collaboration with experimental groups. At the moment it is not clear what kind of experimental set-up will be required. Also it turns out that such resources can be provided by the national or international laboratories only. Therefore, nuclear multfragmentation community has to find out an appropriate form of national and international cooperation right now. Because in a couple of years it will be too late.

Acknowledgements. The fruitful discussions with J. B. Elliott, L. G. Moretto, and L. Phair are appreciated. This work was in part supported by the US Department of Energy.

REFERENCES

1. *Bondorf J. P. et al.* // Phys. Rep. 1995. V. 257. P. 131.
2. *Gross D. H. E.* // Phys. Rep. 1997. V. 279. P. 119.
3. *Moretto L. G. et al.* // Ibid. V. 287. P. 249.
4. For a recent review see: Proc. of the 17th Intern. Conf. on Ultra-Relativistic Nucleus–Nucleus Collisions «Quark Matter 2004», Oakland, California, USA, Jan. 11–17, 2004 // J. Phys. G. 2004. V. 30. P. S633.
5. *Gazdzicki M., Gorenstein M. I.* // Acta Phys. Polon. B. 1999. V. 30. P. 2705; hep-ph/9803462.
6. *Gorenstein M. I., Gazdzicki M., Bugaev K. A.* // Phys. Lett. B. 2003. V. 567. P. 175; hep-ph/0303041.
7. *Yang C. N., Lee T. D.* // Phys. Rev. 1952. V. 87. P. 404.
8. *Chomaz Ph., Gulminelli F.* // Physica A. 2003. V. 330. P. 451.
9. *Hill T. L.* Thermodynamics of Small Systems. N. Y.: Dover Publications, 1994.
10. *Chomaz P., Colonna M., Randrup J.* // Phys. Rep. 2004. V. 389. P. 263.
11. *Gulminelli F. et al.* // Phys. Rev. Lett. 1999. V. 82. P. 1402.
12. *D'Agostino M. et al.* // Phys. Lett. B. 2000. V. 473. P. 219.
13. *Chomaz Ph., Gulminelli F., Duflot V.* // Phys. Rev. E. 2001. V. 64. P. 046114.
14. *Moretto L. G. et al.* // Phys. Rev. C. 2002. V. 66. P. 041601(R).
15. *Moretto L. G., Elliott J. B., Phair L. W.* Mesoscopy and Thermodynamics. Talk given at the conference «World Consensus Initiative III», Texas A&M University, College Station, Texas, USA, Feb. 11–17, 2005; http://cyclotron.tamu.edu/wci3/newer/chapVI_4.pdf
16. *Gyulassy M.* // Lect. Notes Phys. 2002. V. 583. P. 37.
17. *Das Gupta S., Mekjian A. Z.* // Phys. Rev. C. 1998. V. 57. P. 1361.
18. *Das Gupta S. et al.* nucl-th/9903007.
19. *Bugaev K. A. et al.* // Phys. Rev. C. 2000. V. 62. P. 044320; nucl-th/0007062.
20. *Bugaev K. A. et al.* // Phys. Lett. B. 2001. V. 498. P. 144; nucl-th/0103075.
21. *Reuter P. T., Bugaev K. A.* Critical Exponents of the Statistical Multifragmentation Model // Phys. Lett. B. 2001. V. 517. P. 233.
22. *Fisher M. E.* // Physics. 1967. V. 3. P. 255.
23. *Beaulieu L. et al.* // Phys. Lett. B. 1999. V. 463. P. 159.
24. *Elliott J. B. et al. (the EOS Collab.)* // Phys. Rev. C. 2000. V. 62. P. 064603.
25. *Karnaukhov V. A. et al.* // Phys. Rev. C. 2003. V. 67. P. 011601R.
26. *Buyukcizmeci N., Ogul R., Botvina A. S.* nucl-th/0506017 and references therein.
27. *Elliott J. B. et al.* Yield Scalings of Clusters with Fewer than 100 Nucleons. nucl-ex/0608022.
28. *Elliott J. B. et al.* // Phys. Rev. Lett. 2002. V. 88. P. 042701.
29. *Elliott J. B. et al.* // Phys. Rev. C. 2003. V. 67. P. 024609.
30. *Elliott J. B., Moretto L. G., Phair L.* // Phys. Rev. C. 2005. V. 71. P. 024607.
31. *Moretto L. G. et al.* // Phys. Rev. Lett. 2005. V. 94. P. 202701.
32. *Bugaev K. A.* // Acta. Phys. Polon. B. 2005. V. 36. P. 3083.

33. *Bugaev K. A., Phair L., Elliott J. B.* // Phys. Rev. E. 2005. V. 72. P. 047106.
34. *Bugaev K. A., Elliott J. B.* nucl-th/0501080.
35. *Bugaev K. A.* Quark–Gluon Bags with Surface Tension (in preparation).
36. *Gorenstein M. I., Petrov V. K., Zinovjev G. M.* // Phys. Lett. B. 1981. V. 106. P. 327.
37. *Natowitz J. et al.* // Phys. Rev. C. 2002. V. 65. P. 034618.
38. *Elliott J. B. et al. (ISiS Collab.)* // Phys. Rev. Lett. 2002. V. 88. P. 042701.
39. *Yang C. N., Yang C. P.* // Phys. Rev. Lett. 1964. V. 13. P. 303.
40. *Fisher M. E., Felderhof B. U.* // Ann. Phys. 1970. V. 58. P. 217.
41. *Fisher M. E.* // J. Math. Phys. 1964. V. 5. P. 944.
42. *Griffiths R. B.* // J. Chem. Phys. 1965. V. 43. P. 1958.
43. *Liberman D. A.* // J. Chem. Phys. 1966. V. 44. P. 419.
44. *Gilkes M. L. et al.* // Phys. Rev. Lett. 1994. V. 73. P. 1590.
45. *Bauer W., Friedman W. A.* nucl-th/9411012.
46. *Huang K.* Statistical Mechanics. N. Y.: J. Wiley, 1987.
47. *Guida R., Zinn-Justin J.* // J. Phys. Math. Gen. 1998. V. 31. P. 8103.
48. *Elliott J. B., Hirsch A. S.* // Phys. Rev. C. 2000. V. 61. P. 054605.
49. *Das C. B., Das Gupta S., Mekjian A. Z.* // Phys. Rev. C. 2003. V. 68. P. 031601.
50. *Bugaev K. A.* nucl-th/0507028.
51. *Feynman R. P.* Statistical Mechanics. Oxford: Westview Press, 1998.
52. *Gorenstein M. I., Gazdzicki M., Greiner W.* // Phys. Rev. C. 2005. V. 72. P. 024909 and references therein.
53. *Yen G. D., Gorenstein M. I.* // Phys. Rev. C. 1999. V. 59. P. 2788;
Braun-Munzinger P., Heppe I., Stachel J. // Phys. Lett. B. 1999. V. 465. P. 15.
54. *Chodos A. et al.* // Phys. Rev. D. 1974. V. 9. P. 3471.
55. *Gorenstein M. I. et al.* // Teor. Mat. Fiz. 1982. V. 52. P. 346.
56. *Moretto L. G. et al.* // Europhys. Lett. 2006. V. 76. P. 402; LBNL preprint 56898; nucl-th/0504010.
57. *Bugaev K. A. et al.* hep-ph/0504011.
58. *Mader C. M. et al.* // Phys. Rev. C. 2003. V. 68. P. 064601.
59. *Dillmann A., Meier G. E. A.* // J. Chem. Phys. 1991. V. 94. P. 3872.
60. *Kiang C. S.* // Phys. Rev. Lett. 1970. V. 24. P. 47.
61. *Stauffer D., Aharony A.* Introduction to Percolation. Philadelphia: Taylor and Francis, 2001.
62. *Bugaev K. A. et al* // Phys. Lett. B. 2000. V. 485. P. 121.
63. *Bugaev K. A.* nucl-th/0611102.
64. *Heinz U.* nucl-th/0504011.
65. *Bugaev K. A.* // Nucl. Phys. A. 1996. V. 606. P. 559;
Bugaev K. A., Gorenstein M. I. nucl-th/9903072.
66. *Bugaev K. A., Gorenstein M. I., Greiner W.* // J. Phys. G. 1999. V. 25. P. 2147; Heavy Ion Phys. 1999. V. 10. P. 333.

67. *Rischke D. H.* Fluid Dynamics for Reativistic Nuclear Collisions // Proc. of 11th Chris Engelbrecht Summer School in Theoretical Physics: Hadrons in Dense Matter and Hadrosynthesis, Cape Town, South Africa, Feb. 4–13, 1998; nucl-th/9809044.

68. *Bass S. A., Dumitru A.* // Phys. Rev. C. 2000. V. 61. P. 064909.

69. *Teaney D., Lauret J., Shuryak E. V.* // Phys. Rev. Lett. 2001. V. 86. P. 4783; nucl–th/0110037.

70. *Bugaev K. A.* // Phys. Rev. Lett. 2003. V. 90. P. 252301.

71. *Bugaev K. A.* // Phys. Rev. C. 2004. V. 70. P. 034903.